DEVELOPMENT OF HAFF - A HAND WITH ACTIVE FORCE FEEDBACK

by

SHYAMANTA M HAZARIKA

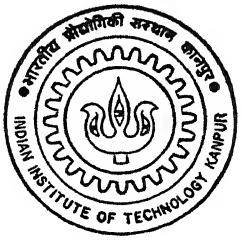

DEPARTMENT OF MECHANICAL ENGINEERING

INDIAN INSTITUTE OF TECHNOLOGY KANPUR

JANUARY, 1996

DEVELOPMENT OF HAFF - A HAND WITH ACTIVE FORCE FEEDBACK

A Thesis Submitted
in Partial Fulfilment of the Requirements
for the Degree of
MASTER OF TECHNOLOGY

by

SHYAMANTA M HAZARIKA

to the

DEPARTMENT OF MECHANICAL ENGINEERING
INDIAN INSTITUTE OF TECHNOLOGY KANPUR
JANUARY, 1996

Certificate

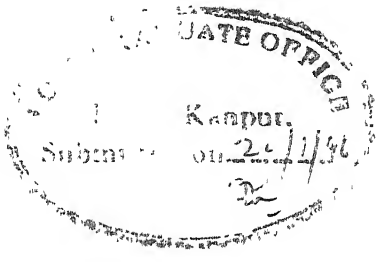

It is certified that the work contained in this thesis entitled "*Development of HAFF - A Hand with Active Force Feedback*" by *Shyamanta M Hazarika*, has been carried out under our supervision and that this work has not been submitted elsewhere for a degree or diploma.

(DR. SUDIPTO MUKHERJEE)
Astt. Professor,
Department of Mechanical Engineering,
Indian Institute of Technology,
Kanpur-208016, INDIA.

(DR. AMITABHA MUKERJEE)
Astt.Professor,
Department of Mechanical Engineering,
Indian Institute of Technology,
Kanpur-208016, INDIA.

Abstract

The problem of grasping by automated hands is often approached with tacit assumptions that the object to be grasped remains stationary and that the fingers can be positioned with perfect control of force and location of every element in contact with the object. Deviating from the above assumptions, the thesis addresses the problem of going from "no-grasp" to "grasp" with impact, for a 2-fingered 4-dof planar hand

In the control strategy for grasping an object, position control of the joints is used to locate the fingertips in proximity of the object. Subsequently, the fingers switch to force control mode. The fingers then accelerate and one of them impacts the object. The object moves forward, propelled by the first finger and comes in contact with the second finger after a finite amount of time delay In other words, during the transistion from "no-grasp" to "grasp", impact generally occurs. We have derived equations to analyze the two impact situations on going from "no-grasp" to "grasp" for a 2-finger 4-dof planar hand

During the course of this work we have designed and developed a 2-fingered 4-dof planar Hand with Active Force Feedback (HAFF) The fingers use strain gauges for force feedback We present a formulation for determining the fingertip forces from strain gauge readings through a matrix estimated for the hand. The complete hardware and the interfacing software for HAFF has been developed.

Acknowledgements

I am grateful to my supervisors Dr.Sudipto Mukherjee and Dr.Amitabha Mukerjee for their unique insight and warm guidance. They have always been encouraging and enthusiastic and it has been a genuiene pleasure working with them Thanks to Dr.Sudipto Mukherjee for his careful reading of this thesis and help me phrase the difficult sections

I would like to thank Mr R.M.Jha for helping me build the hand. Thanks specially to Mr.Prem Gupta who was always ready to machine mechanical parts for the hand. Building and interfacing the planar hand would not have been possible without the support and commitment of Madam Anjali Kulkarni, who was always there to help and make the electronics to work. I would like to extend my heartiest thanks to her. Thanks to Mr.Susmit Sen for guiding me all along, right from the way to hold the soldering-iron to digital control of the motors.

Thanks to all my friends at IIT, Kanpur who have made my stay here valuable, and those at the Center For Robotics for making it a great place to work in. Special thanks to Sharada'da', Manjul'da' and Utpal for their enjoyable company and to Anirvan for many a friutful discussions I had with him during the course of this work.

Above all, my deepest gratitude goes to my parents for their love and support. Thanks to my parents, my sisters Nita'ba' and Rita'ba' and my brother Rupu for their constant encouragement in my endeavour to learn and educate myself.

January 1996,
IIT-Kanpur.

Shyamanta M Hazarika

Contents

List of Figures

Chapter 1

INTRODUCTION

1.1 Introduction

The avenue of coordinated manipulation by multifingered mechanical hands has gained in importance in the area of automated grasping. Versatility of multifingered hands for dexterous and fine manipulation accrues from the fact that they can be used for different objects, objects with large tolerences and objects undergoing change of shape The use of robotic hands obviate the need for custom end effectors.

Literature on multifingered hands has dealt with kinematic design of hands, automatic generation of stable grasping configuration and the use of task requirement as a criterion for selecting grasps. There have been two principal approaches to grasping The first relies on accurate geometric model of the world (Hanafusa and Asada,1977) In the second approach, grasping is accomplished with very little information about the shape of object relying upon primitive behaviors that accomplish somewhat intelligent actions (Chammas,1990). Moreover the problem of grasping (going from "no-grasp" to "grasp") is often approached with tacit assumptions that the object to be grasped remains stationary and that the fingers can be positioned with perfect control of force and location

of every element in contact with the object

Deviating from the above assumptions, the thesis addresses the problem of going from "no-grasp" to "grasp" with impact for a 2-finger 4-dof planar hand Further a 2-fingered 4-dof planar hand has been designed and developed during the course of this work.

1.2 Overview

Grasps are analyzed in terms of "force-closure" or "form-closure" Ohwovoriole (1980) and Salisbury (1982) introduced closure properties in robotic literature Form-Closure originally investigated by Reuleaux (1875) is related to the ability of constraining devices to prevent motion of grasped object, relying only on unilateral frictionless contact constraints. Reuleaux showed that atleast four contact points are necessary to achieve the form-closure property in the planar case and Somov (1900) found that atleast seven are needed in general spatial case. Lakshminarayana (1978) reported about these results.

Analysis of form-closure is intrinsically geometric, in so far as it does not consider the kinematics of the grasping mechanism or the magnitude of the contact forces. Many contributions to form-closure study has been focused on the problem of grasp synthesis (i e given the object geometry place contacts so as to prevent object motions) Baker et al (1985), Mishra et al (1987), Selig and Rooney (1989) and Markenscoff et al (1990) successively discussed the problem of finding form-closure grasps on different surfaces.

A grasp has "force-closure" if any force and couple applied to the object externally can be cancelled by some set of positive forces at the fingers (forces vectors whose inner product with the inward normal to the contacting surface at the point of con-

tact is positive) The synthesis of "force-closure" grasps has been considered by Nguyen (1986) who provided tools for constructing robust force-closure grasp on polyhedral objects Robustness in spite of errors in locating contacts was also a concern of Park and Starr (1992) Ponce et al (1993) extended Nguyen's work to grasp curved 2D objects. Fearing (1986) presented a method for stably grasping 2D polygonal objects with dexterous hand when object models are not available. Markenscoff et al (1988) show that a minimum of three fingers are required to guarantee force closure in the plane, for a piecewise smooth curve For a smooth curve, however, two fingers are sufficient (Chen and Burdick,1992).

Analysis of contact forces and optimization of the grasp in 3D are the next issues and were studied by Kerr and Roth (1986) and Nakamura et al (1989). The technique of finding the efficient force distribution to be commanded have been studied by Kumar and Waldron (1988) and Cheng and Orin (1990). Mukherjee and Waldron (1992) gave an exact optimization for interaction forces in 3-fingered manipulation. Other researchers, such as Holzmann and McCarthy (1985) and Ji and Roth (1988) also focussed on 3-fingered grasping.

The various aspects of kinematics of multifingered mechanical hands have been discussed in depth by Mason and Salisbury (1985). In the literature on grasping and closure analysis, little attention seems to have been paid to the role of end-effector structure and kinematics, with notable exceptions of Trinkle et al (1987), Waldron et al (1989). Pollard and Lozano-Perez (1990) and Hunt et al (1991). Barber et al(1986) presents complete force/moment equations for grasping via a rigid two finger grip.

Research on impact dynamics appears to be scant in comparison to work on grasp synthesis. Even though the physical behaviour of colliding bodies is well established in literature (Goldsmith,1959), research on impact in context of robot manipulators / multi-fingered hands is fairly limited Youcel-Toumi and Li (1987) reported a study of impact under force control Other impact analysis was conducted for legged walking robots interacting with an environment (Zheng et al 1984) Kahng and Amirouche (1987) studied local contact forces associated with impact and gave a derivation for the maximum impact force for a general two-body collision.

A number of articulated hands, such as JPL/Stanford hand (Salisbury,1982), Utah / MIT hand (Jacobsen et al,1985), NYU-FFM (Demmel et al,1988) have been developed to explore problems relating to grasping and manipulation.

1.3 Outline

Chapter 2 reviews the various issues in planar grasping and the the importance of "force-closure" grasps for stable grasping and manipulation.

Chapter 3 investigates collisions involving planar open and closed chains. A practical realisation of these impact situations occur in grasping using two planar fingers We present equations derived to analyse the transition from "no-grasp" to "grasp" for a 2-fingered 4-dof planar hand in this chapter.

Chapter 4 discuss the design and implementation details of a 2-fingered 4-dof planar hand. The entire hardware set-up and the interfacing software is discussed.

Chapter 5 provides a brief review of the thesis. The chapter also enemurates the open problems that remains to be addressed.

Chapter 2

ISSUES IN PLANAR GRASPING

2.1 Introduction

Studies of dexterous robot hands have assumed complete knowledge of object shape, location and orientation This information was used to determine the optimum grasp points and necessary forces for static equilibrium (Salisbury,1982) If such knowledge was not available, grasping strategies were developed, depending on local tactile feedback, object shape constraints and friction forces (Fearing,1986) Construction of independent regions of contact for placing the fingers was put forward (Nguyen,1986). However under noisy object recognition, inexact sensor feedback and inability to position the fingers with perfect control of force and location, there arises the need to explore the viability of the grasping strategies under ambiguity. In the following sections we review the issues in planar grasping and the indispensability of "force-closure" grasp for arriving at stable and manipulable grasp under ambiguity.

We consider objects that can be modelled as prismatic solids. Under the constraints that the objects are restricted to lie on a supporting plane, the problem is reduced to planar motion and forces. Further the finger-object contact is modelled as a single point

contact with friction With this assumption, a finger can apply normal and tangential forces to the object, but no moments.

2.2 Hand Kinematics

A contact between a finger and an object is described by a mapping between forces exerted by the finger at the point of contact and the resultant force and torque at some reference point on the object (say the center of mass) If we have k fingers contacting the object, then the net force on the object is the sum of forces due to each finger The grasp map (also called the Grip transformation) G is the map between finger forces and the resultant object forces.

We represent this map as $6 \times n$ matrix, where n is the number of contact forces generated by the fingers. If F_0 represents the forces and torques exerted on the object in the palm reference frame and f_{c_i} is the force exerted by the i^{th} finger in that same frame, then

$$F_0 = [G_1 + \cdot \cdot + G_k] \begin{bmatrix} f_{c_i} \\ \vdots \\ f_{c_k} \end{bmatrix} = G f_c \qquad (2\ 1)$$

The grip transformation, G, is a function of the position and orientation of the object as well as that of the fingertips

For most grasp situations, equation (2.1) above is underconstrained. The null space of the grasp map corresponds to finger forces which causes no net force to be exerted on the object. We call the forces on the object resulting from finger forces which lie in the null space of G, internal forces. The internal forces allow us to squeeze an object variably, while maintaining equilibrium. In case of planar grasping the force equations

simplify as enumerated in the next section

2.3 Stable Grasp and Graspability

Grasping of planar objects have been analyzed by Fearing (1986), Nguyen (1986), Jacob et al (1990), Chen and Burdick (1992) and a number of other researchers. For a planar object grasped by i fingers, each exerting a force $\vec{f}_{c_i}$, there exists two necessary conditions for a stable grasp First, the object must be in equilibrium i,e the net external force or moment must be balanced by the contact forces.

$$\left.\begin{array}{rcl} \sum \vec{f}_{c_i} & = & \mathbf{F} \\ \sum \vec{r}_i \times \vec{f}_{c_i} & = & \mathbf{M} \end{array}\right\} \tag{2.2}$$

where $\vec{f}_{c_i}$ are the i force vectors and $\vec{r}_i$ are the distance vectors from a fixed point to the each finger $\mathbf{F}$ and $\mathbf{M}$ are the net external force and moment on the object.

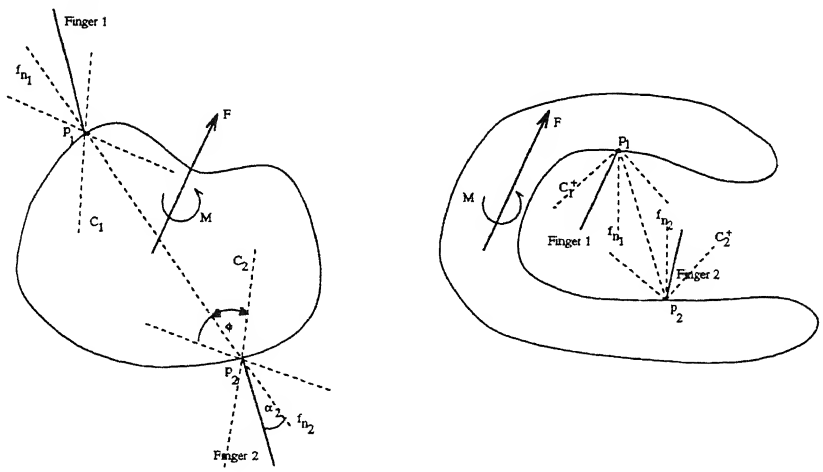

Figure 2 1: Planar Force Closure Grasp

Secondly, for no slip at the fingers, all forces must lie within the cone of friction as in figure 2.1. For grasping using two articulated fingers, the line segment joining the contact

points on the object surface must lie in the friction cones at these points. A friction cone, C_i, at contact point p_i consists of two sectors, one extending outside the object is called the +ve friction cone C^+, the other extending inside the object is called the -ve friction cone C^- Both squeezing grasps where $p_1\bar{p}_2$ falls inside $C_1{}^-$ and $C_2{}^-$, and expanding grasps where $p_1\bar{p}_2$ lies in $C_1{}^+$ and $C_2{}^+$ satisfy force closure conditions A convex body can be grasped by squeezing grasps only Non-convex body can admit both squeezing and expanding grasps

The contact forces have inwardly directed normal components, f_n and component tangent to the boundary f_t The magnitudes F_n and F_t of these forces are governed by the Coulomb inequality.

$$F_n \leq \mu F_t \tag{2.3}$$

where μ is the coefficient of static friction at contact point. Therefore the contact force can make an angle α_i with the normal at point P_i subject to the constraint

$$| \alpha_i | \leq tan^{-1}\mu = \phi_s \tag{2.4}$$

For the condition of graspability, consider the portion of a polygon grasped by two fingers as in figure 2.2. If no external force / moments are acting on the polygon, for equilibrium, the two forces must be colinear, of equal magnitude and opposite sign Therefore, for a polygon, the two force angles cannot be independent, and are related by

$$\alpha_2 = \alpha_1 + \psi \tag{2.5}$$

where ψ is the angle between the surface normals (or in other words the angle between the edges on which the fingers are placed).

Thus for stable grasp of a polygon

$$| \psi | < 2 | \phi_s | \tag{2 6}$$

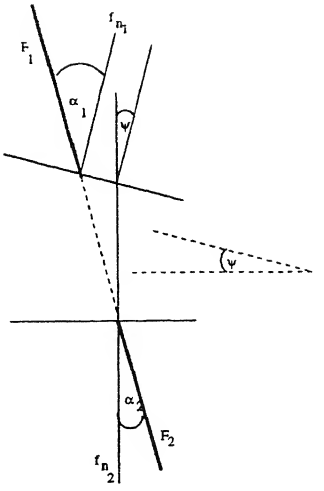

Figure 2.2: Two Finger Grasp of a Polygon

The closer the sides are to being parallel, the smaller the coefficient of friction required to grasp them stably.

2.4 Force Closure - an Underconstrained Problem

The grasping of planar object by two frictional contacts is an underspecified system At each point contact with friction, the magnitude and direction of the force can be controlled. This amounts to two state variables for each finger in the planar case. For two fingers, this amounts to four state variables. There are only three equations, the force balance along orthogonal directions and the moment balance about a fixed point.

Each of the contact forces may act along a direction within a ray centered about the appropiate normal. Intersection of the two rays define a quadrilateral, any point of which

represents a feasible force equilibrium state based on no slip condition as shown in figure 2 3(a)

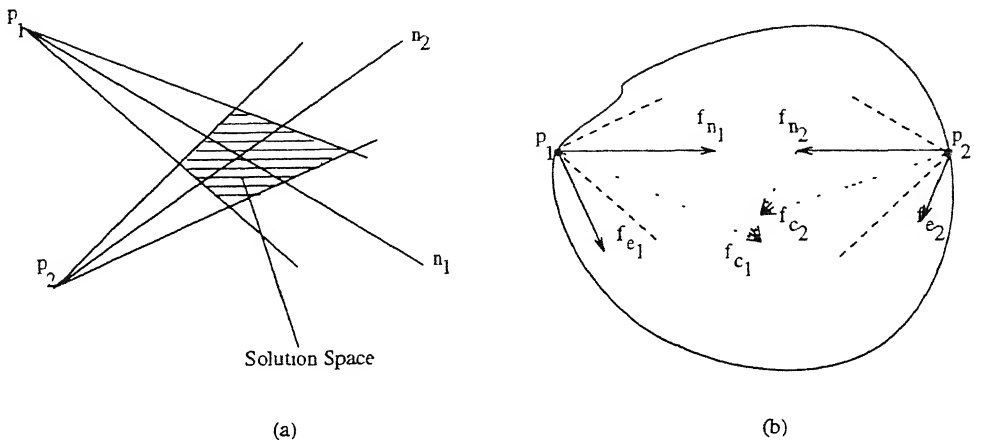

Figure 2 3· Solution space and Nonuniqueness of internal forces

For a given set of equilibrating forces f_{e_i}, selection of appropiate internal forces f_{n_i} can bring the contact force to lie within the solution space as shown in figure 2.3(b) f_{n_i} in two point planar grasp is always two equal and opposite collinear forces. Several researchers have exploited this nonuniqueness of solution, to optimize in accordance with some predetermined criterion (Kerr and Roth,1986, Nakamura et al,1989). Given the uncertainities and inaccuries of the Coulomb model, any criterion based on the minimum values of α_i would be logical.

2.5 Why Force Control ?

The distinction between "form-closure" and "force-closure" is significant in the development of control algorithms for manipulation. Consider the example of a planar polygon, with three frictionless point contacts as shown in figure 2.4

Translational twist space for a single contact

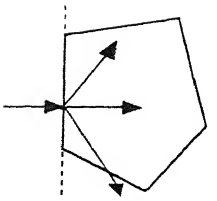

Rotation in CCW direction in half plane above the contact.

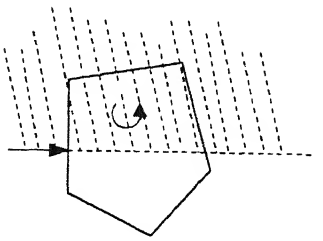

Rotation in CW direction in half plane below the contact.

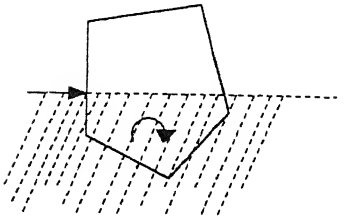

Intersection of rotational space may / maynot be brought to null by a third contact.

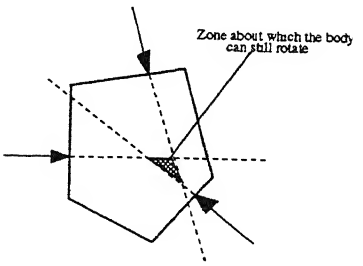

Complete restrain of the body is achieved by bringing the intersection of translational and rotational twist space to null by a fourth contact.

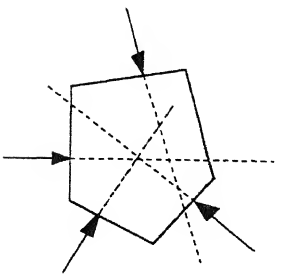

Figure 2.4: Form Closure of a Planar Polygon

At each of the contacts the rotational twist space is partitioned into two half planes The body can have rotations in the clockwise or the counterclockwise directions about points in the two distinct half spaces. Three, or even two contacts can bring the translational twist space to null But the intersection of rotational twist spaces of the contacts is not always null for three contacts and therefore there exists locations about which the body can have rotations In other words the body is not completely restrained, unless a fourth contact is placed such that the intersection of the half spaces is brought to null The contacts now form an opposition. The body cannot move under the influence of applied forces.

For "form-closure" the contacts are assumed to be rigid. This is possible in a multifingered hand if the fingers are controlled in position with very stiff servos Further the "form-closure" theory assumes that all surfaces of the object grasped are available for placement of finger, which ofcourse may not be true in practice. Therefore a stable grasp of a loaded object cannot be guaranteed under form-closure for all loading conditions Also with errors in placement of the fingertips or ambiguity in shape and position of the object, the object may not be completely restrained. There may remain a zone of freedom as shown in figure 2.5.

Contrary to this, in "force-closure", the contacts are not rigid but are, instead, fingers which are controlled to assume a specified contact force. For such a system, the fingers will maintain contact regardless of ambiguity in shape and position of the object and error in placement fingers, unless the contact forces move out of the friction cone. The object may however deviate from the desired trajectory due to the errors.

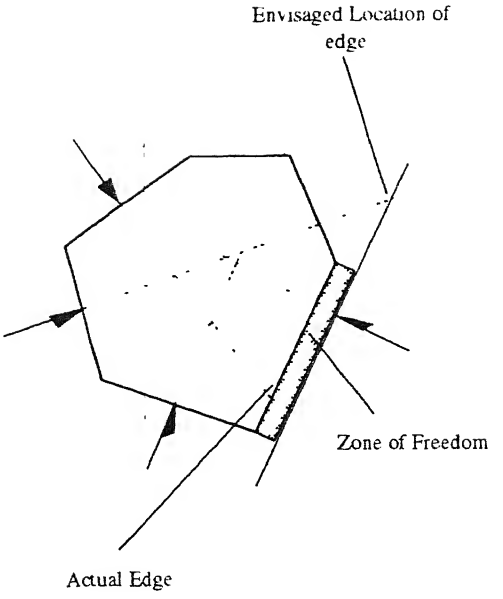

Figure 2.5: Form Closure and ambiguity

The control of a multi-fingered hand during manipulation can be split into two distinct functions. First, the object must be made to follow a desired trajectory and secondly, while doing so the grip on the object should not be lost. If we choose a grasp properly it has been shown that given an arbitrary set of finger forces, f_c, we can find a internal force $f_n \in N(G)$, such that the combined force lies within the friction cone (Cole et al,1988). Thus a force can be generated for the tracking problem and on this we can superimpose the internal force so that the no-slip condition is always satisfied. This makes manipulation under "force-closure" simpler than under "form-closure", which requires the tracking to be done simultaneously maintaining relative position of the fingertips through stiff servo.

Shift from position control mode to the force control mode for acquiring the object under "force-closure" grasp results in impact and consequent motion of the object before being completely grasped. This has been studied in the following chapter.

Chapter 3

IMPACT CLOSURE OF OPEN CHAINS

3.1 Introduction

In this chapter, equations governing collisions involving planar open and closed chains have been developed Two problems have been studied. One problem is that of an open chain impacting an isolated object such that the object attaches itself to the open chain by a revolute joint. The second problem is that of two open chains impacting and forming a closed chain with the object as the additional link. A practical realisation of these two problems occur in grasping using two planar fingers.

A multilinked finger is an open chain mechanism. When one finger makes contact with the object to be grasped, the contact point modelled as point contact with friction, can be treated as a spherical joint (revolute in case of planar mechanisms). The object can subsequently be treated as an additional link added to the open chain. Following which the second finger comes in contact with the object, thus forming a closed chain (as shown in figure 3.1).

In the control strategy for grasping an object, position control of the joints is used to locate the fingertips in proximity of the object. Subsequently, the fingers switch to

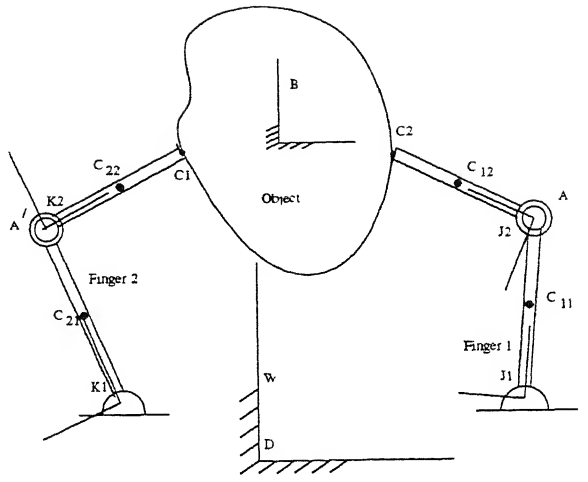

Figure 3.1: The Planar Grasp – a closed chain mechanism.

force control mode. The fingers then accelerate, and one of them impacts the object. The object moves forward, propelled by the first finger, and comes in contact with the second finger after a finite time delay. In other words, during transition from "no-grasp" to "grasp", impact generally occurs.

In this chapter we have derived equations to analyse the two impact situations on going from "no-grasp" to "grasp" for a 2-finger 4-dof planar hand. Simulation of the whole system has been developed on a DEC 300L AXP under X window environment and results presented.

3.2 Grasp Dynamics

This section provides a brief review of dynamics of the fingers. For a more complete discussion see (Sastry et al,1988). These equations combined with the equations derived in section 3.3, form the basis for simulating the 2-finger 4-dof hand, on going from "no -grasp" to "grasp".

3.2.1 Hand Dynamics

The dynamics of a robot manipulator, and in particular a single finger of a hand can be represented as a differential equation with respect to joint angles, θ_i,

$$\mathbf{M}_i(\theta_i)\ddot{\theta}_i + \mathbf{V}_i(\theta_i, \dot{\theta}_i)\dot{\theta}_i + G_i(\theta_i, \dot{\theta}_i) = \tau_i - \mathbf{J}_i{}^T f_c \tag{3 1}$$

where $\mathbf{M}_i(\theta_i) \in R^{n_i \times n_i}$ is the symmetric moment of inertia matrix for the i^{th} finger. $\mathbf{V}_i(\theta_i, \dot{\theta}_i) \in R^{n_i}$ is the vector of Coriolis and centrifugal terms. $G_i(\theta_i, \dot{\theta}_i) \in R^{n_i}$ is the vector of gravity and friction forces. The vector of applied joint torques is $\tau \in R^n$ and $\mathbf{J}_i{}^T f_c$ is the torque due to forces applied at the i^{th} fingertip.

The last term is of considerable significance as it is the presence of this term that causes coupling between the fingers (due to object being grasped). Stacking the equations for all the fingers in the hand we can write the hand dynamics as

$$\mathbf{M}(\Theta)\ddot{\Theta} + \mathbf{V}(\Theta, \dot{\Theta})\dot{\Theta} + G(\Theta, \dot{\Theta}) = \tau - \mathbf{J_h}{}^T f_c \tag{3 2}$$

The dynamics of the object are governed by the Newton-Euler equations. Expressed in the base (inertial) frame, these equations can be written in terms of object position, x_0 and angular velocity, ω_0 w.r.t center of mass.

$$\begin{bmatrix} m_0 I & 0 \\ 0 & I_b \end{bmatrix} \begin{bmatrix} \ddot{x}_0 \\ \dot{\omega}_0 \end{bmatrix} + \begin{bmatrix} 0 \\ \omega_0 \times I_b \omega_0 \end{bmatrix} = \begin{bmatrix} f_0 \\ \tau_0 \end{bmatrix} \tag{3.3}$$

where $m_0 I \in R^{3\times3}$ is the mass matrix for the object and $I_b \in R^{3\times3}$ is the inertia matrix of the object.

In case of planar grasping the object dynamics are somewhat simplified, as the object is only allowed to rotate about an axis perpendicular to plane of motion. If we represent

the position and orientation of the object as (x, y, ϕ) and inertia of object as $I_b \in R$ we have

$$\begin{bmatrix} m_0 & 0 & 0 \\ 0 & m_0 & 0 \\ 0 & 0 & I_b \end{bmatrix} \begin{bmatrix} \ddot{x} \\ \ddot{y} \\ \dot{\phi} \end{bmatrix} = \begin{bmatrix} f_x \\ f_y \\ \tau_\phi \end{bmatrix} \tag{3.4}$$

3.3 Impact Closure

3.3.1 First Impact

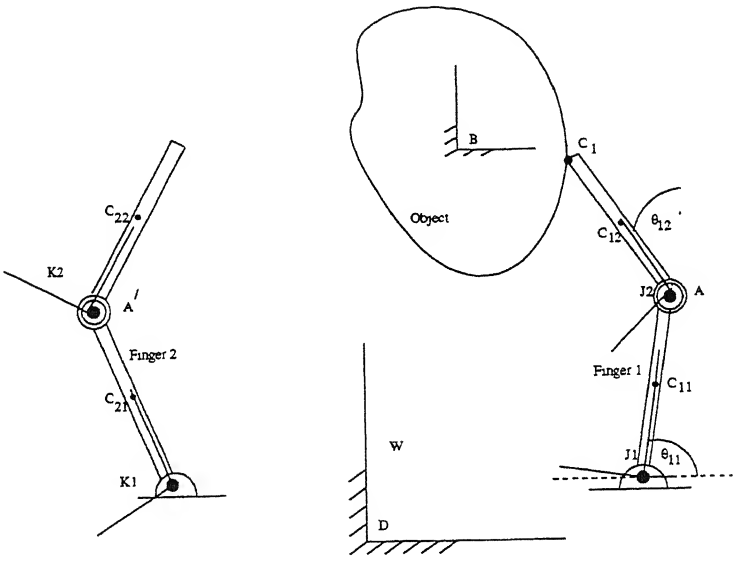

Figure 3.2: Geometry of fingers at first impact

During transition from "no-grasp" to "grasp", the fingertips make contact with the object sequentially due to the inherent error on shifting from position control to force control mode, and impact takes place. There are no prismatic joints in the fingers. Consequently, during impact, torques will not be transmitted across the joints. Internal torques like motor torques are finite ; so their integration over the infinitesimally small duration of

impact can be neglected Therefore, the angular momentum of the selected system will be conserved during impact. Figure 3.2 shows the geometry of first finger, and the object at impact There are four state variables describing the state of the system They are the linear velocity and the angular velocity of the object and the angular velocities of the links of the finger Prior to impact, the state variables are known, and the problem on hand is to compute the values of the four variables after impact.

Angular momemtum conservation of the object being grasped about point C_1 in the world coordinate frame can be represented by the following expression :

$$\mathcal{L}^*_{C_1B} = \mathcal{L}_{C_1B} = \mathcal{L}_{C_B} + (\bar{\mathbf{r}}^W_{C_1B} \times \mathbf{p}^W_B) \tag{3.5}$$

where $\mathcal{L}^*_{C_1B}$ is the angular momentum of the object being grasped about point C_1 before impact, and $\mathcal{L}_{C_B}$ is the angular momentum of the object being grasped about its *center of mass* after impact The vector from point C_1 to point B in the world coordinate frame is $\bar{\mathbf{r}}^W_{C_1B}$ and $\mathbf{p}^W_B$ is the linear momentum of the object being grasped in the world coordinate frame. Unless stated otherwise, terms superscripted with an asterik represents quantities before impact, in the following sections as well.

Point contact with friction is equivalent to replacing the contact between the two bodies with a spherical joint (revolute in case of planar mechanisms). The center of the spherical joint is at the point of contact. Then linear momentum of the object can be written in terms of the velocity of point C_1 and the angular velocity of the object being grasped. Thus equation (3.5) takes the following form :

$$\begin{aligned}\mathcal{L}^*_{C_1B} &= \mathcal{L}_{C_B} + m_b\bar{\mathbf{r}}^W_{C_1B} \times (\bar{\mathbf{v}}^W_{C_1} + \omega_b \times \bar{\mathbf{r}}^W_{C_1B}) \\ &= \mathcal{L}_{C_B} + m_b|\bar{\mathbf{r}}^W_{C_1B}|^2\omega_b + m_b[\bar{\mathbf{r}}^W_{C_1B}\times]\bar{\mathbf{v}}^W_{C_1B}\end{aligned}$$

$$
\begin{aligned}
&= \mathbf{I}_b\omega_b + m_b|\bar{\mathbf{r}}^W_{C_1B}|^2\omega_b + m_b[\bar{\mathbf{r}}^W_{C_1B}\times]\bar{\mathbf{v}}^W_{C_1B} \\
&= \mathbf{M}_{11}\omega_b + m_b[\bar{\mathbf{r}}^W_{C_1B}\times]\mathbf{J}_1\dot{\theta}_1 \\
&= \mathbf{M}_{11}\omega_b + \tilde{\mathbf{a}}_1^T\dot{\theta}_1 \qquad (3.6)
\end{aligned}
$$

where m_b is mass of the object being grasped, ω_b is the angular velocity of the object being grasped and $\bar{\mathbf{v}}^W_{C_1}$ is the velocity of point C_1 in world coordinate frame $\mathbf{J}_1$ is the Jacobian for the first finger, θ_1 is the vector of joint velocities for first finger and $\mathbf{I}_b$ is the moment of inertia of the object being grasped about its center of mass. Further

$$
\begin{aligned}
\tilde{\mathbf{a}}_1^T &= m_b[\bar{\mathbf{r}}^W_{C_1B}\times]\mathbf{J}_1 \\
\mathbf{M}_{11} &= \mathbf{I}_b + m_b|\bar{\mathbf{r}}^W_{C_1B}|^2
\end{aligned}
$$

One additional equation can be generated by considering the angular momentum of object and distal link of the first finger about point A in the world coordiante frame. The following equation is obtained :

$$
\mathcal{L}^*_{A_B} + \mathcal{L}^*_{A_{12}} = (\mathcal{L}_{C_B} + (\bar{\mathbf{r}}^W_{AB} \times \mathbf{p}^W_B)) + (\mathcal{L}_{C_{12}} + (\bar{\mathbf{r}}^W_{AC_{12}} \times \mathbf{p}^W_{12})) \qquad (3.7)
$$

where $\mathcal{L}^*_{A_B}$ is the angular momentum of object being grasped about point A before impact, $\mathcal{L}^*_{A_{12}}$ is the angular momentum of distal link of first finger about point A before impact, $\mathcal{L}_{C_B}$ is the angular momentum of object about its *center of mass* after impact, and $\mathcal{L}_{C_{12}}$ is the angular momentum of distal link about its *center of mass* after impact. The vector from point A to point B in the world coordinate frame is $\bar{\mathbf{r}}^W_{AB}$ and $\bar{\mathbf{r}}^W_{AC_{12}}$ is the vector from point A to *center of mass* of the distal link The linear momentum

of the object being grasped in the world coordinate frame is $\mathbf{p}_B^W$ and $\mathbf{p}_{12}^W$ is the linear momentum of distal link of first finger in the world coordinate frame

Under the assumption of point contact with friction, linear momentum of the object can be expressed in terms of the joint velocities and angular velocity of the object Thus the above equation take the following form :

$$\begin{aligned}
\mathcal{L}^*_{A_{11}} + \mathcal{L}^*_{A_{12}} &= (\mathcal{L}_{C_B} + m_b[\bar{\mathbf{r}}^W_{AB}\times]\bar{\mathbf{v}}^W_b) + (\mathcal{L}_{C_{12}} + m_{12}[\bar{\mathbf{r}}^W_{AC_{12}}\times]\bar{\mathbf{v}}^W_{12}) \\
&= (\mathcal{L}_{C_B} + m_b[\bar{\mathbf{r}}^W_{AB}\times](\bar{\mathbf{v}}^W_{C_1} + \omega_b\times\bar{\mathbf{r}}^W_{C_1B})) \\
&\qquad +(\mathcal{L}_{C_{12}} + m_{12}[\bar{\mathbf{r}}^W_{AC_{12}}\times](\bar{\mathbf{v}}^W_A + \dot{\theta}_{12}\times\bar{\mathbf{r}}^{J2}_{C_{12}})) \\
&= (\mathcal{L}_{C_B} + m_b[\bar{\mathbf{r}}^W_{AB}\times](\mathbf{J}_1\dot{\theta}_1 + \omega_b\times\bar{\mathbf{r}}^W_{C_1B})) \\
&\qquad +(\mathcal{L}_{C_{12}} + m_{12}[\bar{\mathbf{r}}^W_{AC_{12}}\times](\tilde{\mathbf{J}}_1\dot{\theta}_{11} + \dot{\theta}_{12}\times\bar{\mathbf{r}}^{J2}_{C_{12}})) \\
&= (\mathbf{I}_b\omega_b + m_b[\bar{\mathbf{r}}^W_{AB}\times](\mathbf{J}_1\dot{\theta}_1 + \omega_b\times\bar{\mathbf{r}}^W_{C_1B})) \\
&\qquad +(\mathbf{I}_{C_{12}}\dot{\theta}_{12} + m_{12}[\bar{\mathbf{r}}^W_{AC_{12}}\times](\tilde{\mathbf{J}}_1\dot{\theta}_{11} + \dot{\theta}_{12}\times\bar{\mathbf{r}}^{J2}_{C_{12}})) \\
&= \mathbf{M}_{12}\omega_b + \tilde{\mathbf{b}}_1^T\dot{\theta}_1 \qquad (3.8)
\end{aligned}$$

where $\bar{\mathbf{v}}_b^W$ is the velocity of object in the world coordinate frame, $\bar{\mathbf{r}}^{J2}_{C_{12}}$ is the position vector of C_{12} in frame J2, $\mathbf{I}_{C_{12}}$ is the angular momentum of proximal link about its center of mass, $\mathbf{J}_1$ is the Jacobian for the first finger and $\tilde{\mathbf{J}}_1$ is the Jacobian for the proximal link of first finger Further

$$\begin{aligned}
\tilde{\mathbf{b}}_1^T &= [m_b[\bar{\mathbf{r}}^W_{AB}\times]\mathbf{J}_1] + \begin{bmatrix} m_{12}[\bar{\mathbf{r}}^W_{AC_{12}}]\tilde{\mathbf{J}}_1 \\ \mathbf{I}_{C_{12}} + m_{12}[\bar{\mathbf{r}}^W_{AC_{12}}][\bar{\mathbf{r}}^{J2}_{C_{12}}] \end{bmatrix}^T \\
\mathbf{M}_{12} &= \mathbf{I}_b + m_b[\bar{\mathbf{r}}^W_{AB}\times][\bar{\mathbf{r}}^W_{C_1B}]
\end{aligned}$$

Angular momentum of object and the complete finger is then considered about point D in the world coordinate frame. We have the following equation .

$$\mathcal{L}^{\star}_{D_B} + \mathcal{L}^{\star}_{D_{12}} + \mathcal{L}^{\star}_{D_{11}} = (\mathcal{L}_{C_B} + (\bar{\mathbf{r}}^W_{DB} \times \mathbf{p}^W_b)) + (\mathcal{L}_{C_{12}} + (\bar{\mathbf{r}}^W_{DC_{12}} \times \mathbf{p}^W_{12})) + (\mathcal{L}_{C_{11}} + (\bar{\mathbf{r}}^W_{DC_{11}} \times \mathbf{p}^W_{11})) \quad (3\ 9)$$

where $\mathcal{L}^{\star}_{D_B}$ is the angular momentum of object being grasped about point D before impact, $\mathcal{L}^{\star}_{D_{12}}$ is the angular momentum of distal link about point D before impact and $\mathcal{L}^{\star}_{D_{11}}$ is the angular momentum of proximal link about point D before impact. The vector from point D to point B in the world coordinate frame is $\bar{\mathbf{r}}^W_{DB}$, $\bar{\mathbf{r}}^W_{DC_{12}}$ is a vector from point D to *center of mass* of the distal link and $\bar{\mathbf{r}}^W_{DC_{11}}$ is a vector from point D to *center of mass* of the proximal link The linear momentum of distal link in the world coordinate frame is $\mathbf{p}^W_{12}$ and that for the proximal link is $\mathbf{p}^W_{11}$.

In terms of the joint velocities the above equations take the following form

$$\begin{aligned}
\mathcal{L}^{\star}_{D_B} + \mathcal{L}^{\star}_{D_{12}} + \mathcal{L}^{\star}_{D_{11}} &= (\mathcal{L}_{C_B} + m_b[\bar{\mathbf{r}}^W_{DB}\times]\mathbf{v}^W_b) + (\mathcal{L}_{C_{12}} + m_{12}[\bar{\mathbf{r}}^W_{DC_{12}}\times]\mathbf{v}^W_{12})) \\
&\quad +(\mathcal{L}_{C_{11}} + [\bar{\mathbf{r}}^W_{DC_{11}}\times]\mathbf{v}^W_{11})) \\
&= [\mathcal{L}_{C_B} + m_b[\bar{\mathbf{r}}^W_{DB}\times](\mathbf{v}^W_{C_1} + \omega_b \times \bar{\mathbf{r}}^W_{OB})] \\
&\quad +[\mathcal{L}_{C_{12}} + m_{12}[\bar{\mathbf{r}}^W_{DC_{12}}\times](\mathbf{v}^W_A + \dot{\theta}_{12} \times \bar{\mathbf{r}}^{J2}_{C_{12}})] \\
&\quad +[\mathcal{L}_{C_{11}} + m_{11}[\bar{\mathbf{r}}^W_{DC_{11}}\times](\dot{\theta}_{11} \times \mathbf{r}^{J1}_{C_{11}}) \\
&= [\mathbf{I}_b\omega_b + m_b[\bar{\mathbf{r}}^W_{DB}\times](\mathbf{v}^W_{C_1} + \omega_b \times \bar{\mathbf{r}}^W_{OB})] \\
&\quad +[\mathbf{I}_{C_{12}}\dot{\theta}_{12} + m_{12}[\bar{\mathbf{r}}^W_{DC_{12}}\times](\mathbf{v}^W_A + \dot{\theta}_{12} \times \bar{\mathbf{r}}^{J2}_{C_{12}})] \\
&\quad +[\mathbf{I}_{C_{11}}\dot{\theta}_{11} + m_{11}[\bar{\mathbf{r}}^W_{DC_{11}}\times](\dot{\theta}_{11} \times \mathbf{r}^{J1}_{C_{11}})
\end{aligned}$$

$$= \mathbf{M}_{13}\omega_b + \tilde{\mathbf{d}_1}^T\dot{\theta}_1 \qquad (3\ 10)$$

where $\bar{\mathbf{r}}_{C_{11}}^{J1}$ is the position vector of *center of mass* of proximal link in frame J1 The term $\mathbf{I}_{C_{11}}$ is the momemt of inertia of proximal link of first finger about its *center of mass* Further

$$\begin{aligned}
\mathbf{M}_{13} &= \mathbf{I}_b + m_b[\bar{\mathbf{r}}_{DB}^W\times]\bar{\mathbf{r}}_{C_1B}^W \\
\tilde{\mathbf{d}_1}^T &= m_b[\bar{\mathbf{r}}_{DB}^W\times]\mathbf{J}_1 + \begin{bmatrix} m_{12}[\bar{\mathbf{r}}_{DC_{12}}^W\times]\tilde{\mathbf{J}}_1 + \mathbf{I}_{C_{11}} + m_{11}[\bar{\mathbf{r}}_{DC_{11}}^W\times][\bar{\mathbf{r}}_{C_{11}}^{J1}] \\ \mathbf{I}_{C_{12}} + m_{12}[\bar{\mathbf{r}}_{DC_{12}}^W\times][\bar{\mathbf{r}}_{C_{12}}^{J2}] \end{bmatrix}^T
\end{aligned}$$

Concatenating equations (3.6),(3.8) and (3.10), we determine the angular velocity ω_b of the object and joint velocity vector $\dot{\Theta}_1$ of the first finger after contact with the object being grasped, from the following equation

$$\begin{bmatrix} \tilde{\mathbf{a}}_{11} & \tilde{\mathbf{a}}_{12} & \mathbf{M}_{11} \\ \tilde{\mathbf{b}}_{11} & \tilde{\mathbf{b}}_{12} & \mathbf{M}_{12} \\ \tilde{\mathbf{d}}_{11} & \tilde{\mathbf{d}}_{12} & \mathbf{M}_{13} \end{bmatrix} \begin{Bmatrix} \dot{\theta}_{11} \\ \dot{\theta}_{12} \\ \omega_b \end{Bmatrix} = \begin{Bmatrix} \mathcal{L}_{C_1}^* \\ \mathcal{L}_A^* \\ \mathcal{L}_D^* \end{Bmatrix} \qquad (3.11)$$

Once ω_b and $\dot{\Theta}_1$ is determined using the above equation, velocity of the object after first impact is given as

$$\left.\begin{aligned} \bar{\mathbf{v}}_b^W &= \bar{\mathbf{v}}_{C_1}^W + \omega_b \times \bar{\mathbf{r}}_{C_1B}^W \\ &= \mathbf{J}_1\dot{\Theta}_1 + \omega_b \times \bar{\mathbf{r}}_{C_1B}^W \end{aligned}\right\} \qquad (3\ 12)$$

3.3.2 Second Impact

After the first impact, the object is propelled by the first finger and comes in contact with the second finger after a finite time delay. The system now becomes a closed chain. Figure 3.3 shows the geometry at the second impact.

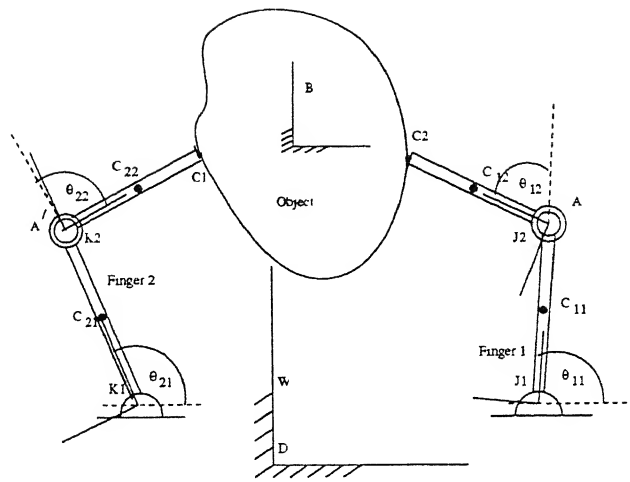

Figure 3 3· Geometry of fingers at second impact.

Conservation of angular momentum in the world coordinate frame, for the complete system, comprising of the two fingers and the object being grasped, yeilds the following equation:

$$\begin{aligned}\mathcal{L}^*_W = \quad & (\mathcal{L}_{C_{11}} + \bar{\mathbf{r}}^W_{DC_{11}} \times \mathbf{p}^W_{11}) + (\mathcal{L}_{C_{12}} + \bar{\mathbf{r}}^W_{DC_{11}} \times \mathbf{p}^W_{12}) \\ & +(\mathcal{L}_{C_B} + \bar{\mathbf{r}}^W_{DB} \times \mathbf{p}^W_B) \\ & +(\mathcal{L}_{C_{21}} + \bar{\mathbf{r}}^W_{DC_{21}} \times \mathbf{p}^W_{21}) + (\mathcal{L}_{C_{22}} + \bar{\mathbf{r}}^W_{DC_{22}} \times \mathbf{p}^W_{22})\end{aligned} \tag{3.13}$$

$$\begin{aligned}\mathcal{L}^*_W &= \begin{bmatrix} m_b[\bar{\mathbf{r}}^W_{DB}] \\ \mathbf{I}_b \end{bmatrix} \begin{Bmatrix} \mathbf{v}_{\mathbf{b}x} \\ \mathbf{v}_{\mathbf{b}y} \\ \omega_b \end{Bmatrix} + \begin{bmatrix} (\mathbf{I}_{C_11} + m_{11}[\bar{\mathbf{r}}^W_{DC_{11}}\times][\bar{\mathbf{r}}^{J1}_{C_{11}}] \\ \qquad +m_{12}[\bar{\mathbf{r}}^W_{DC_{12}}\times]\mathbf{J}_1) \\ \mathbf{I}_{C_12} + m_{12}[\bar{\mathbf{r}}^W_{DC_{12}}\times][\bar{\mathbf{r}}^{J2}_{C_{12}}] \\ (\mathbf{I}_{C_21} + m_{21}[\bar{\mathbf{r}}^W_{DC_{21}}\times][\bar{\mathbf{r}}^{K1}_{C_{21}}] \\ \qquad +m_{22}[\bar{\mathbf{r}}^W_{DC_{22}}\times]\mathbf{J}_2) \\ \mathbf{I}_{C_22} + m_{22}[\bar{\mathbf{r}}^W_{DC_{22}}\times][\bar{\mathbf{r}}^{K2}_{C_{22}}] \end{bmatrix}^T \begin{Bmatrix} \dot{\theta}_{11} \\ \dot{\theta}_{12} \\ \dot{\theta}_{21} \\ \dot{\theta}_{22} \end{Bmatrix} \\ &= \mathbf{M}_{21}\mathcal{V} + \tilde{\mathbf{a}_2}^T\dot{\Theta}\end{aligned} \tag{3.14}$$

where $\mathcal{L}^*_W$ is the angular momentum of the system in world coordinate before impact,

$\mathcal{V}$ is the generalized velocity vector of the object $= \left\{ \begin{array}{cccc} \bar{\mathbf{v}}_{b_x} & \bar{\mathbf{v}}_{b_y} & \omega_b \end{array} \right\}^T$, and

Θ is the vector of joint velocities for the fingers $= \left[\begin{array}{cc} \dot{\Theta}_1 & \dot{\Theta}_2 \end{array} \right]^T$

The other two equations are obtained by representing the contact forces in terms of change in angular momentum We select a point B', as shown in figure 3 4

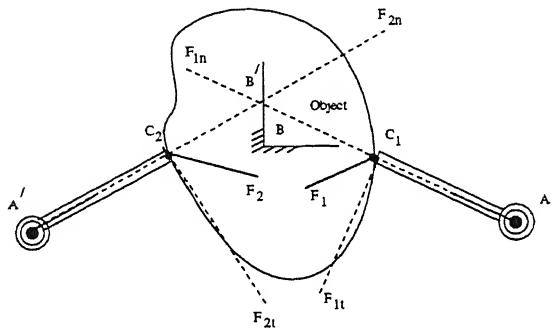

Figure 3.4: Location of point B' in world frame.

Angular momentum change about point B', because of forces acting on the object being grasped due to contacts at C_1 and C_2 is given by the following equation :

$$\begin{aligned} \mathcal{L}_{B'_b} - \mathcal{L}^*_{B'_b} &= \bar{\mathbf{r}} \times \int \mathcal{F}\, \partial t \\ &= \int (|\bar{\mathbf{r}}^{B'}_{C_1}| \mathcal{F}_{1t} + |\bar{\mathbf{r}}^{B'}_{C_2}| \mathcal{F}_{2t})\, \partial t \end{aligned} \tag{3 15}$$

where $\mathcal{L}_{B'_b}$ is the angular momentum of the object about point B', and $\mathcal{L}^*_{B'_b}$ is the angular momentum of the object about point B' before impact. $\mathcal{F}_{1t}$ is the tangential component

of force on the object through contact C_1 and $\mathcal{F}_{2t}$ is the tangential component of force on the object through contact C_2 The position vector of contact point C_1 in frame B' is $\bar{\mathbf{r}}_{C_1}^{B'}$ and $\bar{\mathbf{r}}_{C_2}^{B'}$ is the position vector of contact point C_2 in frame B'. The point B' has been selected so that the normal components of the impact forces do not figure in the equations of momentum conservation about point B'.

For distal link of first finger

$$\begin{aligned} \delta\mathcal{L}_{12} &= \bar{\mathbf{r}}_{C_1}^{J2} \times \int \mathcal{F}_1 \, \partial t \\ &= |\bar{\mathbf{r}}_{C_1}^{J2}| \int \mathcal{F}_{1t} \, \partial t \\ \int \mathcal{F}_{1t} \, \partial t &= \frac{\mathcal{L}_{B'_{12}} - \mathcal{L}^*_{B'_{12}}}{|\bar{\mathbf{r}}_{C_1}^{J2}|} \end{aligned} \tag{3.16}$$

and distal link of second finger

$$\begin{aligned} \delta\mathcal{L}_{22} &= \bar{\mathbf{r}}_{C_2}^{K2} \times \int \mathcal{F}_2 \, \partial t \\ &= |\bar{\mathbf{r}}_{C_2}^{K2}| \int \mathcal{F}_{2t} \, \partial t \\ \int \mathcal{F}_{2t} \, \partial t &= \frac{\mathcal{L}_{B'_{22}} - \mathcal{L}^*_{B'_{22}}}{|\bar{\mathbf{r}}_{C_2}^{K2}|} \end{aligned} \tag{3.17}$$

where $\delta\mathcal{L}_{12}$ is the angular momentum change of distal link of first finger about B', $\delta\mathcal{L}_{22}$ is the angular momentum change of distal link of second finger about B', $\bar{\mathbf{r}}_{C_2}^{J2}$ is the position vector of contact point C_1 in frame J2, $\bar{\mathbf{r}}_{C_2}^{K2}$ is the position vector of contact point C_1 in frame K2

Introducing equations (3.16) and (3.17) in equation (3.15) above, we have the following expression

$$\mathcal{L}_{B'_b} - \mathcal{L}^*_{B'_b} = |\bar{\mathbf{r}}_{C_1}^{B'}| \frac{\mathcal{L}_{B'_{12}} - \mathcal{L}^*_{B'_{12}}}{|\bar{\mathbf{r}}_{C_1}^{J2}|} + |\bar{\mathbf{r}}_{C_2}^{B'}| \frac{\mathcal{L}_{B'_{12}} - \mathcal{L}^*_{B'_{12}}}{|\bar{\mathbf{r}}_{C_2}^{K2}|} \tag{3.18}$$

Let $a_1 = \frac{|\mathbf{r}_{C_1}^{B'}|}{|\mathbf{r}_{C_1}^{J2}|}$ and $a_2 = \frac{|\bar{\mathbf{r}}_{C_2}^{B'}|}{|\bar{\mathbf{r}}_{C_2}^{K2}|}$ then we have

$$\begin{aligned}
\mathcal{L}_{B'_b} - \mathcal{L}^*_{B'_b} &= a_1(\mathcal{L}_{B'_{12}} - \mathcal{L}^*_{B'_{12}}) + a_2(\mathcal{L}_{B'_{22}} - \mathcal{L}^*_{B'_{22}}) \\
\mathcal{L}^*_{B'_b} - a_1\mathcal{L}^*_{B'_{12}} - a_2\mathcal{L}^*_{B'_{22}} &= \mathcal{L}_{B'_b} - a_1\mathcal{L}_{B'_{12}} - a_2\mathcal{L}_{B'_{22}} \\
\mathcal{L}^*_{B'} &= \mathcal{L}_{B'_b} - a_1\mathcal{L}_{B'_{12}} - a_2\mathcal{L}_{B'_{22}} \\
&= [(\mathbf{I}_b\omega_b + m_b\bar{\mathbf{r}}_b^{B'} \times \bar{\mathbf{v}}_b^W) \\
&\quad -a_1(\mathbf{I}_{C_{22}}\dot{\theta}_{22} + m_{22}\bar{\mathbf{r}}_{C_{22}}^{B'} \times \bar{\mathbf{v}}_{C_{22}}) \\
&\quad -a_2(\mathbf{I}_{12}\dot{\theta}_{12} + m_{12}\bar{\mathbf{r}}_{C_{12}}^{B'} \times \bar{\mathbf{v}}_{C_{12}}) \qquad (3\ 19)
\end{aligned}$$

On simplification the above equation reduces to :

$$\begin{aligned}
\mathcal{L}^*_{B'} &= \begin{bmatrix} m_b[\bar{\mathbf{r}}_b^{B'}\times] \\ \mathbf{I}_b \end{bmatrix}^T \mathcal{V} - \begin{bmatrix} a_1 m_{12}[\bar{\mathbf{r}}^{B'}\times]\tilde{\mathbf{J}}_1 \\ a_1(\mathbf{I}_{12} + m_{12}[\bar{\mathbf{r}}_{C_{12}}^{B'}\times][\bar{\mathbf{r}}_{C_{12}}^{J2}] \\ a_2 m_{22}[\bar{\mathbf{r}}_{C_{22}}^{B'}\times]\tilde{\mathbf{J}}_2 \\ a_2(\mathbf{I}_{C_{22}} + m_{22}[\bar{\mathbf{r}}_{C_{22}}^{B'}\times][\bar{\mathbf{r}}_{C_{22}}^{K2}]) \end{bmatrix}^T \dot{\Theta} \\
&= \mathbf{M}_{22}\mathcal{V} + \tilde{\mathbf{b}_2}^T\Theta \qquad (3\ 20)
\end{aligned}$$

We choose point B'' as shown in figure 3.5 for the next equation Angular momentum change about B'' because of the contact forces at C_1 and C_2 is given as

$$\begin{aligned}
\mathcal{L}_{B''_b} - \mathcal{L}^*_{B''_b} &= \bar{\mathbf{r}} \times \int \mathcal{F}\,\partial t \\
&= \int (|\bar{\mathbf{r}}_{C_1}^{B''}|\mathcal{F}_{1t} + |\bar{\mathbf{r}}_{C_2}^{B''}|\mathcal{F}_{2t})\,\partial t \qquad (3.21)
\end{aligned}$$

For first finger

$$\delta\mathcal{L}_{F1} = \bar{\mathbf{r}}_{C_1}^{J1} \times \int \mathcal{F}_1\,\partial t$$

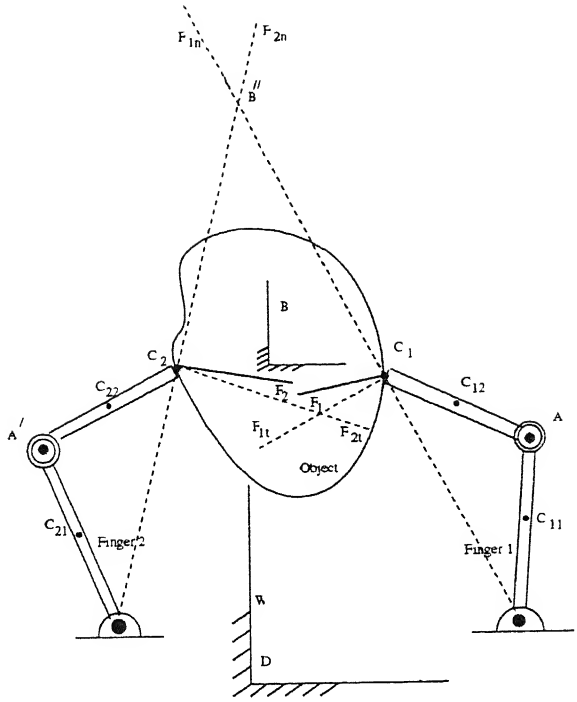

Figure 3 5 Location of point B'' in world frame.

$$\begin{aligned} &= |\bar{\mathbf{r}}_{C_1}^{J1}| \int \mathcal{F}_{1t}\, \partial t \\ \int \mathcal{F}_{1t}\, \partial t &= \frac{\mathcal{L}_{B''_{F1}} - \mathcal{L}^*_{B''_{F1}}}{|\bar{\mathbf{r}}_{C_1}^{J1}|} \end{aligned} \tag{3.22}$$

and for the second finger

$$\begin{aligned} \delta\mathcal{L}_{F2} &= \bar{\mathbf{r}}_{C_2}^{K1} \times \int \mathcal{F}_2\, \partial t \\ &= |\bar{\mathbf{r}}_{C_2}^{K1}| \int \mathcal{F}_{2t}\, \partial t \\ \int \mathcal{F}_{1t}\, \partial t &= \frac{\mathcal{L}_{B''_{F2}} - \mathcal{L}^*_{B''_{F2}}}{|\bar{\mathbf{r}}_{C_2}^{K1}|} \end{aligned} \tag{3 23}$$

where $\delta\mathcal{L}_{F1}$ is the change in angular momentum about B'' for first finger, $\delta\mathcal{L}_{F2}$ is the change in angular momentum about B'' for second finger, $\bar{\mathbf{r}}_{C_2}^{K1}$ is the position vector of contact point C_2 in frame K1.

Introducing equations (3 22) and (3.23) in (3.21) we have the following expression

$$\mathcal{L}_{B''_b} - \mathcal{L}^*_{B''_b} = \frac{|\bar{\mathbf{r}}_{C_1}^{B''}|}{|\bar{\mathbf{r}}_{C_1}^{J1}|}(\mathcal{L}_{B''_{F1}} - \mathcal{L}^*_{B''_{F1}}) + \frac{|\bar{\mathbf{r}}_{C_2}^{B''}|}{|\bar{\mathbf{r}}_{C_2}^{K1}|}(\mathcal{L}_{B''_{F2}} - \mathcal{L}^*_{B''_{F2}}) \tag{3 24}$$

Let $d_1 = \frac{|\mathbf{r}_{C_1}^{B''}|}{|\bar{\mathbf{r}}_{C_1}^{J1}|}$ and $d_2 = \frac{|\mathbf{r}_{C_2}^{B''}|}{|\bar{\mathbf{r}}_{C_2}^{K1}|}$ then we have

$$\begin{aligned} \mathcal{L}_{B_b''} - \mathcal{L}^{\star}_{B_b''} &= d_1(\mathcal{L}_{B''_{F1}} - \mathcal{L}^{\star}_{B''_{F1}}) + d_2(\mathcal{L}_{B''_{F2}} - \mathcal{L}^{\star}_{B''_{F2}}) \\ \mathcal{L}^{\star}_{B_b''} - d_1(\mathcal{L}^{\star}_{B''_{F1}}) - d_2(\mathcal{L}^{\star}_{B''_{F2}}) &= \mathcal{L}_{B_b''} - d_1(\mathcal{L}_{B''_{F1}}) - d_2(\mathcal{L}_{B''_{F2}}) \end{aligned} \tag{3 25}$$

On further simplification equation (3 25) reduces to

$$\begin{aligned} \mathcal{L}^{\star}_{B''} &= \mathcal{L}_{B_b''} - d_1(\mathcal{L}_{B_{11}''} + \mathcal{L}_{B_{12}''}) - d_2(\mathcal{L}_{B_{21}''} + \mathcal{L}_{B_{22}''}) \\ &= \begin{bmatrix} m_b[\bar{\mathbf{r}}_b^{B''}\times] \\ \mathbf{I}_b \end{bmatrix}^T \mathcal{V} - \begin{bmatrix} d_1(\mathbf{I}_{11} + m_{11}[\bar{\mathbf{r}}_{C_{11}}^{B''}\times][\bar{\mathbf{r}}_{C_{11}}^{J1}] + m_{12}[\bar{\mathbf{r}}_{C_{12}}^{B''}\times]\tilde{\mathbf{J}}_1) \\ d_1(\mathbf{I}_{12} + m_{12}[\bar{\mathbf{r}}_{C_{12}}^{B''}\times][\bar{\mathbf{r}}_{C_{12}}^{J2}]) \\ d_2(\mathbf{I}_{21} + m_{21}[\bar{\mathbf{r}}_{C_{21}}^{B''}\times][\bar{\mathbf{r}}_{C_{21}}^{K1}] + m_{22}[\bar{\mathbf{r}}_{C_{22}}^{B''}\times]\tilde{\mathbf{J}}_2) \\ d_2(\mathbf{I}_{C_{22}} + m_{22}[\bar{\mathbf{r}}_{C_{22}}^{B''}\times][\bar{\mathbf{r}}_{C_{22}}^{K2}]) \end{bmatrix}^T \Theta \\ &= \mathbf{M}_{23}\mathcal{V} + \tilde{\mathbf{d}_2}^T\dot{\Theta} \end{aligned} \tag{3.26}$$

As discussed in 3.3.1 point contact with friction can be envisaged as a spherical joint with its center at the point of contact, the contact point velocity can be related to the body velocity Because of the contact constraint the velocity of the contact points C_1 and C_2 in the coordinate frame of the object being grasped is zero i.e

$$\begin{aligned} \mathbf{v}_{C_1}^B &= 0 \\ \mathbf{v}_{C_2}^B &= 0 \end{aligned}$$

Expressing the velocity of the contact points in the world coordinate frame we have the following expressions

$$\begin{aligned} \mathbf{v}_{C_1}^W &= \mathbf{v}_{B_{origin}}^W + \mathbf{R}_B^W \mathbf{v}_{C_1}^B \\ &= \mathbf{J}_1 \dot{\Theta}_1 = \bar{\mathbf{v}}_b^W \end{aligned} \tag{3 27}$$

$$\begin{aligned} \mathbf{v}_{C_2}^W &= \mathbf{v}_{B_{origin}}^W + \mathbf{R}_B^W \mathbf{v}_{C_2}^B \\ &= \mathbf{J}_2 \dot{\Theta}_2 = \bar{\mathbf{v}}_b^W \end{aligned} \tag{3 28}$$

The above equations can be put in the following canonical form

$$\hat{\mathbf{R}} \mathcal{V} + \mathbf{J}_h \dot{\Theta} = 0 \tag{3 29}$$

where

$\hat{\mathbf{R}}$ = 4 × 3 matrix of the form = $\begin{bmatrix} -1 & 0 & 0 \\ 0 & -1 & 0 \\ -1 & 0 & 0 \\ 0 & -1 & 0 \end{bmatrix}$

$\mathbf{J}_h$ = Jacobian for both the fingers = $\begin{bmatrix} \mathbf{J}_1 & 0 \\ 0 & \mathbf{J}_2 \end{bmatrix}$

Finally concatenating equations (3.14), (3.20), (3.26) and (3.29) we have the following canonical form

$$\begin{bmatrix} \mathbf{M} & \mathbf{A} \\ \hat{\mathbf{R}} & \mathbf{J}_h \end{bmatrix} \begin{bmatrix} \mathcal{V} \\ \dot{\Theta} \end{bmatrix} = \begin{bmatrix} \mathcal{L}^* \\ 0 \end{bmatrix} \tag{3 30}$$

where,

$\mathbf{A}$ is the 3 × 4 matrix of momentum coefficients = $\begin{bmatrix} \tilde{\mathbf{a}_2}^T & \tilde{\mathbf{b}_2}^T & \tilde{\mathbf{d}_2}^T \end{bmatrix}^T$,

$\mathbf{M}$ is the 3 × 3 matrix of mass and inertia terms = $\begin{bmatrix} \mathbf{M}_{21} & \mathbf{M}_{22} & \mathbf{M}_{23} \end{bmatrix}^T$, and

$\mathcal{L}^*$ is the 3 × 1 vector of momentum terms before grasp.

The generalized velocity of the object being grasped and the joint velocities of both the fingers, after the second impact can be computed from equation (3.30).

3.4 Simulation Results

The results of the simulation on going from "no-grasp" to "grasp" using a 2-finger 4-dof planar hand is presented There are two revolute joints on each finger The lengths of the proximate and distal links are 8.0 and 6 5 cm respectively. The thickness of the links has been neglected Further the contact being point contact with friction, sliding motion has not been considered in this simulation. The geometry of the grasped object is a circular disc of 5 0 cm diameter. During the grasping operation, the palm of the hand is kept stationary.

For this illustrative example, the object is placed so as to have a forward english after impact The plots of the angular velocity of the object and the links of the fingers are shown in figure 3 7 Animation pictures, are plotted based on the results of the numerical simulation process Three frames showing the position and orientation of the object and the fingers at different instants are shown in figure 3.6, for the forward english imparted at the first impact.

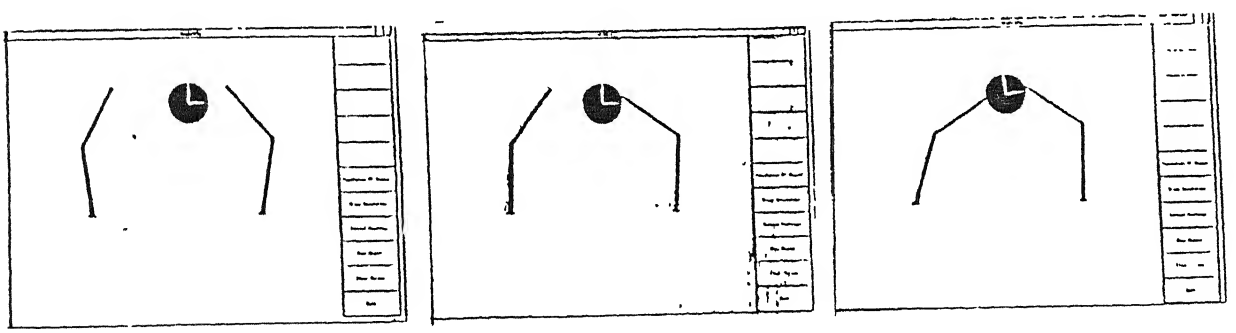

Figure 3.6· Animation pictures at different instants

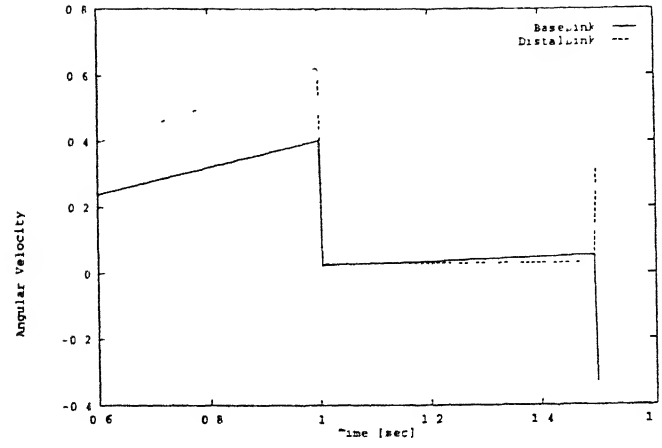

Angular velocities for links of the first finger.

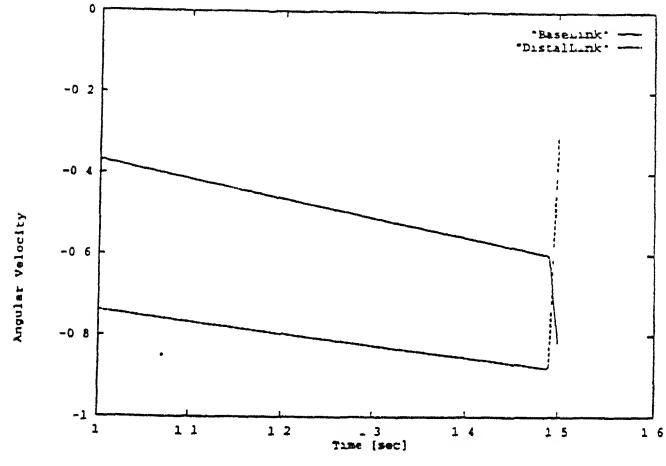

Angular velocities for links of the second finger.

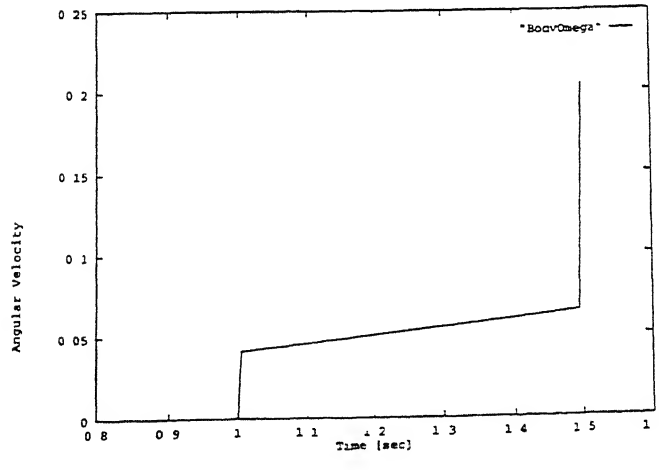

Angular velocity of the body

Figure 3.7: Plots ofAngular velocity of finger links and object

The first impact takes place after 1 sec from the start At the first impact, angular velocities of both the links of the first finger drops Thereafter it increases, but at a very slow rate At the second impact, that takes place after 0 5 seconds from the first impact, the second finger makes contact with the object at a point below its center of mass The object's angular velocity takes a sharp rise in the counterclockwise direction as expected. The change in sign of the angular velocity of the distal link of the second finger and the sharp rise in case of the base link is as expected, as the joint between the links, for the given configuration, have a tendency to cave-in during the impact. The changes in the angular velocity of the links of the first finger is because of the tendency of the joint to cave-out at the second impact

The formulation can be put to use for predicting the joint velocities and the generalized velocity of the object after grasp This can be used for initial correction of the trajectory in fine manipulation.

Chapter 4

HAFF - AN IMPLEMENTATION

4.1 Introduction

During the course of this work we have built a 2-fingered 4-dof planar hand. In this chapter we present the design and implementation details of the planar hand The entire hardware set-up can be divided into two broad categories :

a. The mechanical components of the planar hand

and b Drive and Control Electronics.

The control is through the printer port of a PC-AT 386. In the following sections we also discuss the interfacing software.

4.2 Overview of HAFF

The planar hand comprises of two multi-linked fingers. As shown in figure 4.1, each finger of HAFF consists of two links. The individual links are designed as slotted bars. Apppendix D has detailed drawings of the fingers. Each link is directly driven by a DC motor The driver motor of the distal link is mounted on the base link. The base link is supported by a roller mounted at right angles to the link to take up the weight. The base

link is driven by a motor fixed to the frame. Two identical pair of fingers placed a fixed distance apart constitutes HAFF. The placement of the finger can be changed with the workspace requirement of the hand.

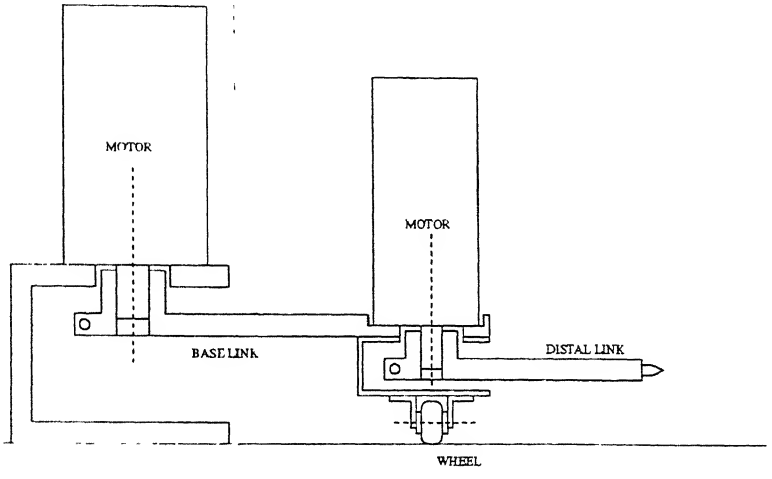

Figure 4.1: Schematic of a finger

Optical encoders on the motors give the position feedback of the fingers A pair o resistance wire strain gauges are mounted at the base of each link. The force feedback through these strain gauges In appendix A we present a formulation for determining th fingertip forces based on strain gauge readings using a matrix that can be estimated fo the given hand

4.3 Drive and Control Electronics

The drive and control hardware comprises of the following units :

a Motor driver boards.

b Strain Gauge bridge circuitry.

c. PCLD-789 Amplifier / Multiplexer Board

and d PCL-208 High Performance Data Acquisition Card.

4.3.1 Motor Driver Boards

The motor driver circuit implements the configuration given in figure 4.2. The circuit was not designed as part of this work. A description has been included for completeness It consists of two sets of identical switches SW1 / SW2 and SW3 / SW4 realized through transistors The complete circuit diagram is given in appendix B. Two such driver circuits are placed on a single motor driver board.

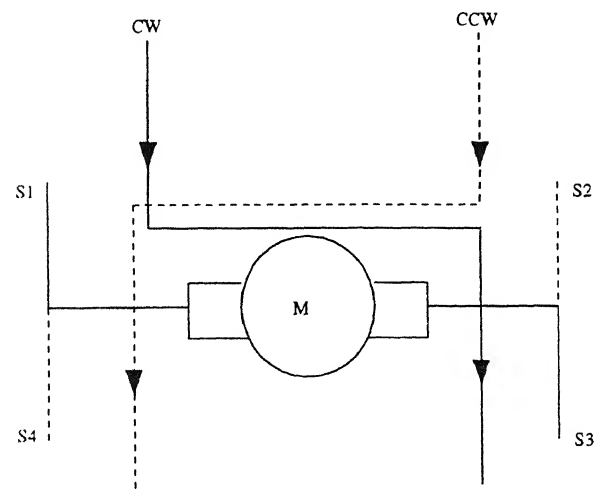

Figure 4.2: Directional Switching of a motor

The following explanation is with respect to motor A. The control signals for BAF and BAR are supplied by pulses (logic levels 0V = LOW ; 5V = HIGH) through the printer port of a PC-AT by software control. Input of the NAND gate is passed on to

the output when the protection bit, P, is high, with output being the inverted input. At any instant, if motor A is rotating clockwise, the following logic level must prevail

$$P = \text{HIGH},\ BAF = \text{HIGH},\ BAR = \text{LOW}$$

$$\text{Then } N1_{output} = N4_{output} = HIGH$$

$$N2_{output} = N3_{output} = LOW$$

The high NAND outputs make the concerned transistors ON, where as the others remain OFF Thus for the above logic levels transistors T1 and T4 are OFF, and T2 and T3 are ON As a result the collector current flows through the transistors T2 and T3, which causes their collector potential to go low The opposite is the case with other two transistors T1 and T4. Of the darlington pairs, D1 and D2 are the NPN type and D3 and D4 are PNP type The ON/OFF status of the darlington pairs depend on the corresponding states of the transistors The transistor ON/OFF states for forward and reverse rotation of the motors are given in Table 4 1

Rotation	BAF	BAR	T_1	D_1	T_2	D_2	T_3	D_3	T_4	D_4
Forward	H	L	OFF	ON	ON	OFF	ON	ON	OFF	OFF
Reverse	L	H	ON	OFF	OFF	ON	OFF	OFF	ON	ON

Table 4 1. Transistor states for direction of rotation of a motor

Each motor driver board has two such controller Therefore a pair of such boards is used for driving the four joints of the hand Further, following the above discussion, AF, AR and BF, BR are the two sets of control bits (to each driver board) for two motors, to decide the direction of current flow Logic Table 4.2 shows the corresponding motor status A 50 core flat cable is used and both the driver boards are daisy chained to

the printer port Appendix C shows the connector pin assignment along with the port address and corresponding bits for the different motors.

Forward	Reverse	Motor Status
0	0	NOP
0	1	CCW
1	0	CW
1	1	NOP

Table 4.2 Logic Table for Motor Status

4.3.2 Strain Gauge Bridge Circuitry

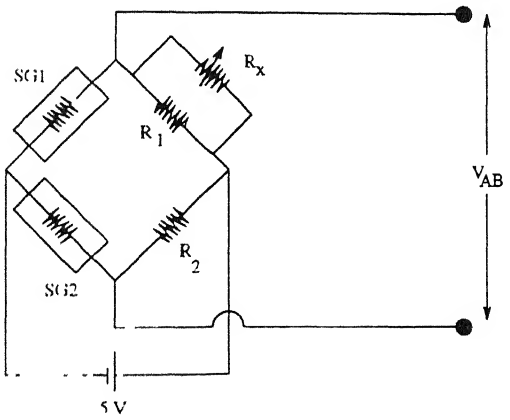

Figure 4.3: Strain Gauge Bridge Circuitry

The Wheatstone bridge shown in figure 4.3 is used to detect the change in resistance of the strain gauges Each pair of resistance wire strain gauges placed at the base of each of the links forms adjacent arms of the bridge. Four such circuits are cascaded together to form the complete strain gauge circuitry. Appendix C gives the complete pin diagram for the strain gauges input and differential output to PCLD-789 from the board

Figure 4.3 also shows the use of a balancing (zero adjust) potentiometer, R_x. It is highly unlikely that the resistors chosen to complete the bridge will be exactly equal to the resistance of the strain gauge or to each other. Because the bridge is required to be sensitive to very small changes in resistane, the bridge must initially be balanced The balancing potentiometer is used to adjust the bridge output voltage to zero when the gauge is unstrained. The values of the balancing potentiometer and the resistor in parallel are chosen so that the voltage at point A may be raised or lowered, since the initial imbalance could have either polarity Hence R_1 must be larger than the other resistances (which are 120 Ω each) , so that when R_x is large, their parallel combination yields a value that is also larger than 120 Ω and lowers V_A. When R_x is adjusted to be small, the resulting parallel combination is smaller than 120 Ω and raises V_A. A single potentiometer could have been used instead of the parallel combination of R_1 and R_x; however, the resolution would have been poor and fine adjustments would have been very difficult.

4.3.3 PCLD-789 : Amplifier / Multiplexer Board

Analog to digital conversion of the differential voltage of the Wheatstone bridge is carried out inside the PC-AT 386 using PCL-208, a standard PCL series data acquisition card However, it requires voltage signals in a particular range to be applied to the input channels of the ADC cards The differential voltage from the strian gauge bridge being of the order of μV, the signal needs to be amplified before it can be fed to the input channel of the ADC card. Amplification of the differential input signal is done through the PCLD-789 card, which has instrumentation amplifiers with a range of gain selections. We work with a gain of 1000.

The PCLD-789 has 16 differential inputs, out of which currently the first four are only being used for reading the output of the four pair of strain gauges. The channel selection is done through the TTL output pins of the PCL-208 card being used for interfacing. Other software requirements are dictated by the ADC card being used, because the PCLD-789 does not take part in any other software manipulations except for multiplexing the desired channels and connecting the selected input to the output.

4.3.4 PCL-208 : Data Acquisition Card

The PCL-208 card is used for analog to digital conversion The card supports 16 single-ended or 8 differential analog inputs configuration As the output from PCLD-789 is a single-ended signal, we use the +/- 5.0 V single-ended input range. This is switch selectable, using different jumper settings. For more details refer to the Owner's Manual PCL-208.

The PCL-208 uses 12 bit A/D conversions, and an 8 bit register is not enough to accommodate all 12 bits of data. Therefore A/D data is stored in two registers located at address BASE + 0 and + 1. Through software, we suitably convert it to a single number, to refer to a particular voltage output.

4.4 Software Outline

PC-AT 386 uses vectored imterrupts. Whenever a device interrupts the processor, it is responsible for telling the CPU which interrupt service routine should be executed. The software for interfacing and control make use of the vectored interrupts. In order to obtain a real time signal, the timer tick interrupt of PC-AT 386 is used The timer tick interrupt

at vector $1C_{hex}$ comes 18.2 times per sec This is because the standard bus clock signal of 2 38 MHz is first divided by 2 and then by $(2^{16} - 1)$, as the divisor latch (internal to the clock) is loaded by $(2^{16} - 1)$ Since this rate of timer tick interrupt is too small, the divisor latch is loaded by the FINGER software with $256_{decimal}$ to obtain exactly 4648 real time interrupts per sec All events, sampling, delays etc are subsequently timed by this clock The interrupt service also keeps track of the motor encoder pulse transitions.

The FINGER software comprises of three basic modules, which are interweaved into each other and in a strict sense do not form independent units. The three basic modules are the following :

a Position Control Module

b. Force Feedback Module

and c Force Control Module.

4.4.1 Position Control Module

The voltage input to the motors are controlled through pulse width modulation. In appendix A we present details on pulse width modulation. In conjunction with the optical encoder feedback, the position control of the motors is achieved The position control module for the motors involves the following steps :

Step 1 · Get optical encoder feedback and decide direction of motion of the motor. There -after increment/decrement a variable (count).

Step 2 : Determine difference between desired position (position) and the present value of count.

For position > count - move motor in forward direction.

For position < count - move motor in reverse direction.

Step 3 · Repeat steps 1 through 3 for (position - count) $\neq$ 0

4.4.2 Force Feedback Module - A/D Conversion

The force feedback is through the strain gauges mounted at the base of the finger links The complete A/D operation for reading in the differential voltage of the strain gauges using software trigger involves the following steps :

Step 1 : Set input channel by specifying the scan range.

Step 2 : Trigger by writing to the A/D low byte register (BASE + 0) with any value

Step 3 : Wait for End Of Conversion by reading the A/D status register (BASE + 8)

Step 4 : Read data from A/D converter by reading the A/D data registers.

Step 5 · Data conversion by converting the binary A/D data to an integer.

4.4.3 Force Control Module

The force control and the force feedback module work in close coordination The fingertip forces are gauged by the strain gauge readings and the duty cycle of the motors changed accordingly to approach the desired values. The force control module involves the following steps .

Step 1 : From the fingertip force vector computed (using the matrix formulation in appendix A) determine the difference between the desired and the actual force.

Step 2 . Compute the unit vector along which the applied torque is required to change

to arrive at the desired force, using the following equations

$$\mathbf{J}^T \triangle F_c = \triangle \tau$$

$$\triangle \hat{u} = \triangle \tau / \mid \triangle \tau \mid$$

where $\triangle F_c$ is the error in the fingertip force and $\mathbf{J}$ is the jacobian of the finger $\triangle \tau$ is the required difference in torque and $\triangle \hat{u}$ is the unit vector along the desired direction

Step 3 · The ratio of ON time to the time period of pulses (δ) is computed using the following expression

$$\delta_{i+1} = \delta_i + \alpha \triangle \hat{u}$$

where $\alpha = k \triangle F_c$ and k the is desired gain.

Chapter 5

CONCLUSION

5.1 Review

In this thesis we have reviewed grasping by a planar hand. During the course of this work we have also built a 2-fingered 4-dof planar hand.

Chapter 1 serves as an introduction to this thesis and present an overview of the area of multifingered manipulation

Chapter 2 reviews the issues in planar grasping and the indispensability of "force-closure" grasps for arriving at stable and manipulable grasp under ambiguity of parameters

In Chapter 3, without going into the assumption that the object to be grasped remains stationary during the transition from "no-grasp" to "grasp", we derive equations to analyze the impact situations for a 2-fingered 4-dof planar hand.

Chapter 4 describes the complete hardware and interfacing software for the 2-fingered 4-dof hand.

5.2 Open Problems

While we have derived equations which govern the motion of the object after impact on going from "no-grasp" to "grasp", several areas of investigation needs to be persued for physically achieving grasp under impact and uncertainity in placing the fingertips

Control Scheme

For a two finger planar grasp, even after the second contact, the object has a tendency to continue its angular rotation under its momentum A control scheme to bring the angular velocity of the object to zero after the second impact needs to be developed This could be the immediate extension of this work.

Grasping under Ambiguity

Under noisy object recognition, inexact sensor feedback and inability to position the fingers with perfect control of force and location, there arises the need to explore the validity of the grasping strategies under ambiguity. For this ambiguity needs to be modelled into the system and robust grasping strategies developed.

Appendix A

A.1 Force Estimation from Strain Gauge Readings

We determine the fingertip forces from the strain gauge readings using a matrix, the coefficients of which are experimentally estimated for the given finger.Figure A.1 shows the freebody diagram for the links of a single finger.

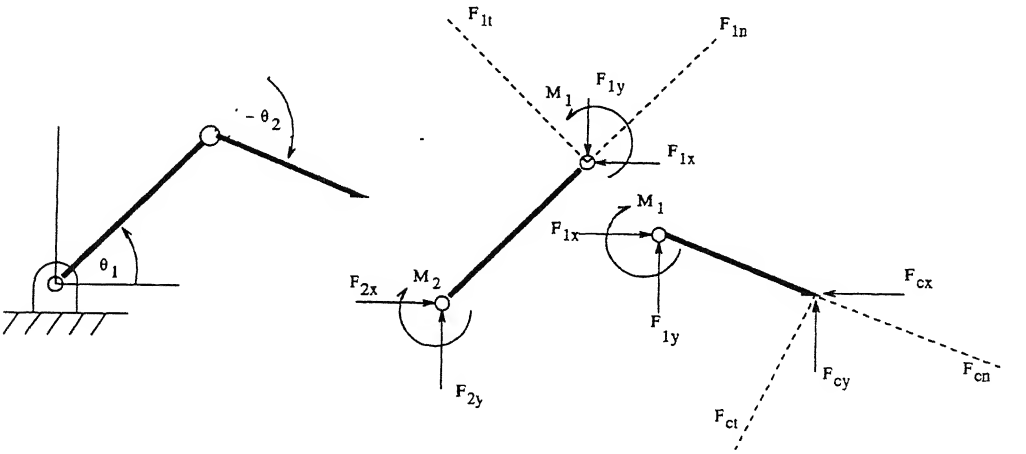

Figure A.1: Freebody Diagram of Finger Links

For distal link, equating the forces and moments, we have

$$F_{1x} - F_{cx} = 0$$

$$F_{1y} - F_{cy} = 0$$

$$-M_1 + F_{cy} l_1 c_{12} - F_{cy} l_1 s_{12} = 0$$

The above equations can be put in the matrix form as

$$\begin{Bmatrix} F_{1x} \\ F_{1y} \\ M_1 \end{Bmatrix} = \begin{bmatrix} 1 & 0 \\ 0 & -1 \\ -l_1 s_{12} & -l_1 c_{12} \end{bmatrix} \begin{Bmatrix} F_{cx} \\ F_{cy} \end{Bmatrix} \quad \text{(A 1)}$$

For base link, using a transformation to bring the forces along normal and tangential directions :

$$\begin{Bmatrix} F_{1n} \\ F_{1t} \\ M_1 \end{Bmatrix} = \begin{bmatrix} c_1 & s_1 & 0 \\ -s_1 & c_1 & 0 \\ 0 & 0 & 1 \end{bmatrix} \begin{Bmatrix} F_{1x} \\ F_{1y} \\ M_1 \end{Bmatrix} \quad \text{(A 2)}$$

Considering the finger links as cantilevers the strain at the gauges can be estimated. The strain is given as $\epsilon = \frac{My}{EI}$ and the total moment at the strain gauge is given as

$$\begin{aligned} M &= -F_{1t}\delta_2 + M_1 \\ &= -(-s_1 F_{1x} + F_{1y} c_1)\delta_2 + M_1 \end{aligned}$$

Introducing equations (A.1) and (A.2) into the above equation yields

$$\begin{aligned} M &= (F_{cx} s_1 + F_{cy} c_1)\delta_2 - F_{cx} l_1 s_{12} + F_{cy} l_1 c_{12} \\ &= (\delta_2 s_1 - l_1 s_{12}) F_{cx} + (\delta_2 c_1 + l_1 c_{12}) F_{cy} \end{aligned}$$

Strain developed in the strain gauges of the base links is :

$$\epsilon_1 = (k_1 s_1 - k_2 s_{12}) F_{cx} + (k_1 c_1 + k_2 c_{12}) F_{cy} \quad \text{(A.3)}$$

where, $k_1 = \frac{y}{EI}\delta_2$ and $k_2 = \frac{yl_1}{EI}$

and strain developed in the strain gauges of the distal links is :

$$\epsilon_2 = -k_3 s_{12} F_{cx} + k_3 c_{12} F_{cy} \tag{A.4}$$

where, $k_3 = \frac{y\delta_1}{EI}$ The differential voltage across the strain gauges is proportional to the strain i.e. $V_{AB} \propto \epsilon$. Hence differential voltage for the base link is

$$\begin{aligned} V_{AB_1} &= \mathbf{G}\epsilon_1 \\ &= \mathbf{G}[(k_1 s_1 - k_2 s_{12})F_{cx} + (k_1 c_1 + k_2 c_{12})F_{cy}] \\ &= (a_1 s_1 - a_2 s_{12})F_{cx} + (a_1 c_1 + a_2 c_{12})F_{cy} \end{aligned} \tag{A.5}$$

and that for the distal link is given as

$$\begin{aligned} V_{AB_2} &= \mathbf{G}\epsilon_2 \\ &= \mathbf{G}[-k_3 s_{12} F_{cx} + k_3 c_{12} F_{cy}] \\ &= a_3 s_{12} F_{cx} + a_3 c_{12} F_{cy} \end{aligned} \tag{A.6}$$

Concatenating the above equations, we have the following canonical form

$$\begin{aligned} \begin{Bmatrix} V_{AB_1} \\ V_{AB_2} \end{Bmatrix} &= \begin{bmatrix} a_1 s_1 - a_2 s_{12} & a_1 c_1 + a_2 c_{12} \\ a_3 s_{12} & a_3 c_{12} \end{bmatrix} \begin{Bmatrix} F_{cx} \\ F_{cy} \end{Bmatrix} \\ \bar{V}_{AB} &= \mathbf{A}\bar{F}_c \end{aligned}$$

The coefficients of the matrix **A** can be estimated for the hand. The fingertip forces can then be determined from the following expression.

$$\bar{F}_c = \mathbf{A}^{-1}\bar{V}_{AB} \tag{A.7}$$

A.2 Pulse Width Modulation

A basic switching regulator consists of four major components as shown in figure A.2 :

a Voltage Source V_{in}

b Switch S_1

c Pulse Generator V_{pulse}

and d Filter F_1

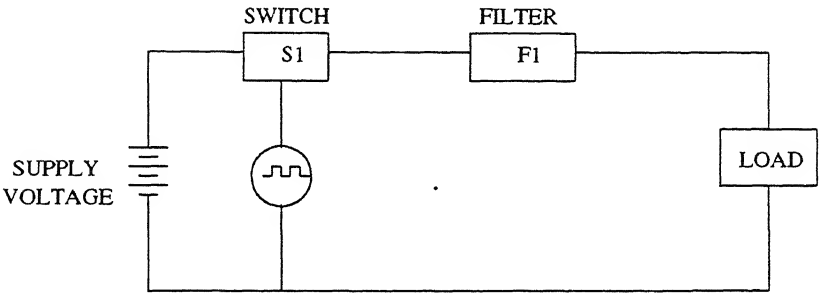

Figure A 2: Pulse Width Modulation

Voltage source , V_{in}, may be any D.C supply. It must supply the required output power and losses associated with the switching regulator. It must have the capacity to supply sufficient dynamic range voltage for line and load variations.

Switch S_1, is typically a transistor connected as a power switch and is operated in the saturated mode The pulse generator output alternately turns the switch ON and OFF.

Pulse generator, V_{pulse}, produces an asymmetric square wave as shown in figure A.3 varying in pulse width. The duty cycle of the pulse waveform determines the relationship

between the input and output voltage. Duty cycle is the ratio of ON time, t_{on},to the period T of the pulse waveform. The output voltage, V_{out}, of the switching regulator is a function of duty cycle and the input voltage V_{in}.

$$V_{out} = V_{in}(t_{on}/(t_{on} + t_{off})) \tag{A.8}$$

where, t_{on} is the ON time of the pulse waveform and t_{off} is the OFF time of the pulse waveform.

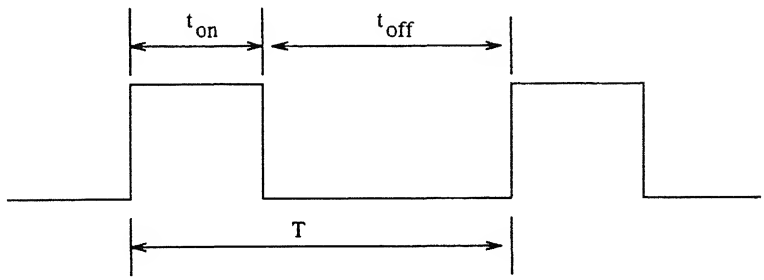

Figure A.3: Duty cycle in a square waveform

If the time period T is constant, the output voltage, V_{out} is directly proportional to the ON time, t_{on}, for a given value of V_{in}. This method of changing the output voltage by varying t_{on} is referred to as Pulse Width Modulation

Appendix B

B.1 Driver Board Circuit Diagram

B.1.1 Driver Circuit

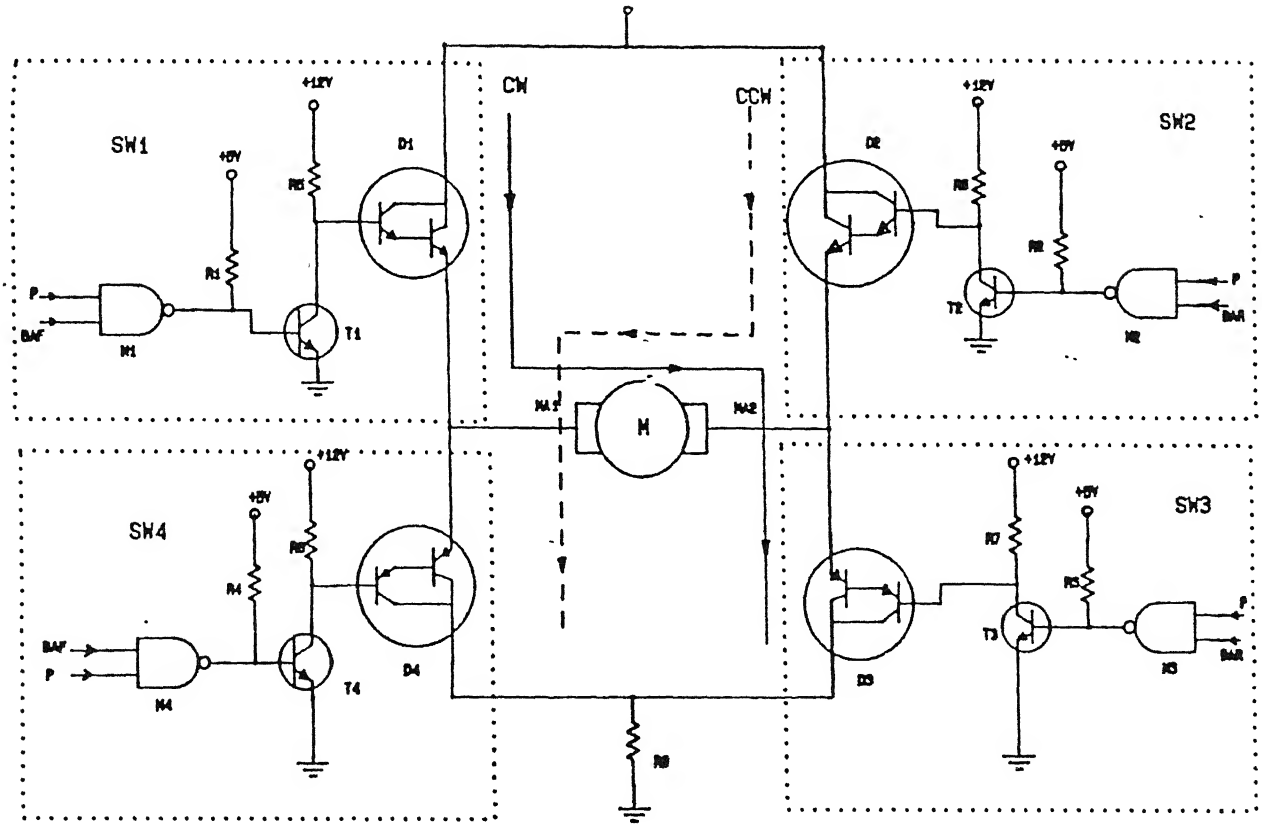

B.1.2 Printer Port to Driver Circuit

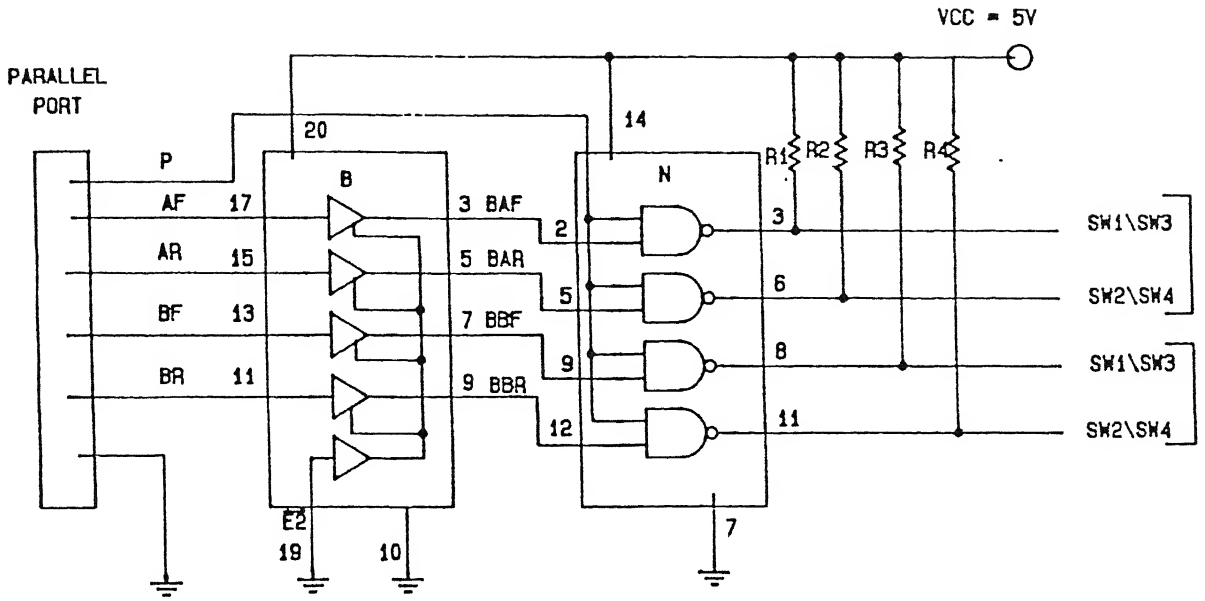

Electronic Components List

B	74LS244 OCTAL BUFFER LINE DRIVER
N	74LS38 OPEN COLLECTOR NAND
T1, T2, T3, T4	SL100 NPN TRANSISTORS
D1, D2	BD677 NPN DARLINGTON PAIR
D3, D4	BD678 PNP DARLINGTON PAIR
R1, R2, R3, R4	4.7 kohm
R5, R6, R7, R8	1 kohm

Appendix C

C.1 Driver Board and Printer Port Connections

Signal	*50 Pin FRC (Driver Board)*	*25 Pin D-type (Printer Port)*		
		Pin	Port	Bit
PROT	1	1	X7A	0
AFOR	3	2	X78	0
CFOR	5	3	X78	1
AREV	11	4	X78	2
CREV	13	5	X78	3
BFOR	19	6	X78	4
DFOR	21	7	X78	5
BREV	27	8	X78	6
DREV	29	9	X78	7
SELAB	35	14	X7A	1
SELCD	37	16	X7A	2
BOPTA1	43	10	X79	7
BOPTA2	45	11	X79	6
BOPTB1	47	12	X79	5
BOPTB2	49	13	X79	4
GND	2,4, $\cdots$ 50	18, $\cdots$ 25		

C.2 Strain Gauge Circuit Board Connections

Input 20 pin FRC		*Output 20 pin FRC*		
SG 1	*SG 2*	V_A	V_B	*AGND*
1,2	3,4	2	4	1,3
5,6	7,8	6	8	5,7
9,10	11,12	10	12	9,11
13,14	15,16	14	16	13,15

C.3 Motor to Driver Board Connections

9 Pin D-type	*Motor Cable*
1	Motor Power +ve
3	Encoder Power +ve
6	Encoder Signal 1
8	Encoder Signal 2
9	Motor Power -ve

Appendix D

D.1 Detail Drawing of the Fingers

D.1.1 Proximal Link

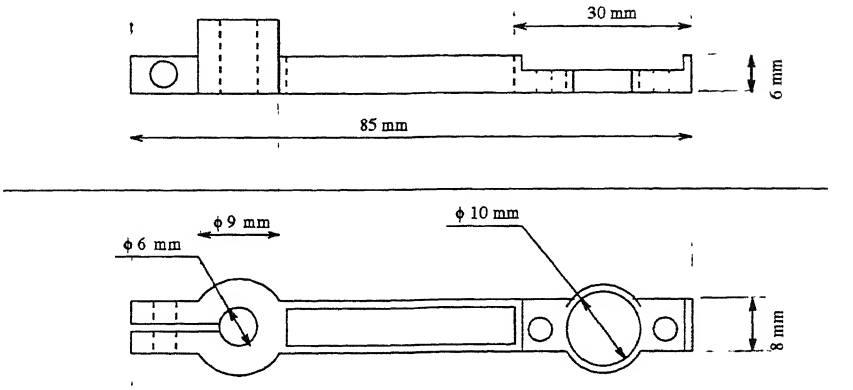

D.1.2 Distal Link

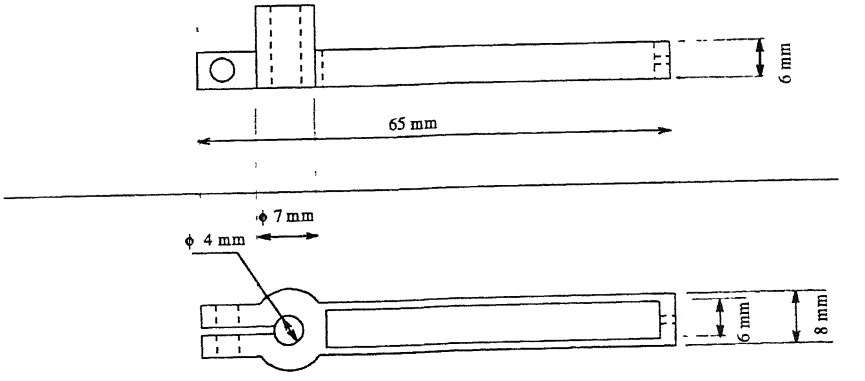

Bibliography

[1] **Baker,B.S., Fortune,S.** and **Grosse,E.**, 1985. Stable Prehension with a Multifingered Hand . Proc. of IEEE Int. Conf. on R and A ; pp. 570-575.

[2] **Barber,J., Volz,R.A.** and **Desai,R.**, 1986. Automatic Two Fingered Grip Selection . Proc of IEEE Int. Conf. on R and A ; pp. 870-896.

[3] **Bicchi,A.**, 1995. On the Closure Properties of Robotic Grasping . Int. J. of Robotics Res., Vol 14(4) ; pp. 319-334.

[4] **Brost,C.R.**, 1985. Planning Robot Grasping motions in presence of Uncertainity . CMU-RI, Technical Report 85-12, CMU, Pittsburgh.

[5] **Chammas,C.Z.**, 1990. Analysis and Implementation of Robust Grasping behaviours . MIT AI Lab, Technical Report 1237, MIT, Cambridge.

[6] **Chen,I.M.** and **Burdick,J.W.**, 1992. Finding Antipodal Point Grasps on Irregularly Shaped Objects . Proc. of IEEE Int. Conf. on R and A ; pp. 2278-2283.

[7] **Cheng,F.T.** and **Orin,D.E.**, 1990. Efficient Algorithm for Optimal force distribution - the compact dual LP method . IEEE J. of R and A, Vol 6(2) ; pp. 178-187.

[8] **Cole,A.**, **Hauser,J.** and **Sastry,S.**, 1988. Kinematics and Control of Multifingered Hands with rolling contact . Proc. of IEEE Int. Conf. on R and A ; pp. 228-233.

[9] **Cutkowsky,M.R.**, 1985. Robotic Grasping and Fine Manipulation . Kluwer Academic Publishers, Boston.

[10] **Faverjon,B.** and **Ponce,J.**, 1991. On Computing Two Finger Force Closure Grasps of Curved 2D objects . Proc of IEEE Int Conf. on R and A ; pp. 424-429.

[11] **Fearing,R.S.**, 1986. Simplified Grasping and Manipulation with dextrous robot hands IEEE Int. J of R and A, Vol 2(4) ; pp. 188-195.

[12] **Goldsmith,W.**, 1959. Impact : The Theory and Physical Behaviour of Colliding Solids . Edward Arnold Publishers, London.

[13] **Hanafusa,H.** and **Asada,H.**, 1977. Stable Prehension by a robot hand with elastic fingers . Proc. Int. Symp. on Industrial Robots ; pp. 311-368.

[14] **Hollerbach,J.** and **Narasimhan,S.**, 1986. Finger Force Computation without the Grip Jacobian . Proc. of IEEE Int. Conf. on R and A ; pp. 871-875.

[15] **Holzmann,W.** and **McCarthy,J.M.**, 1985. Computing the Friction Forces associated with a 3-fingered grasp . IEEE J. of R and A, Vol 1(4) ; pp. 206-210.

[16] **Hunt,K.H.**, **Samuel,A.E.** and **McAree,P.R.**, 1991. Special configurations of multi-finger multi-freedom grippers - a kinematic study . Int. J of Robotics Res., Vol 10(2) ; pp. 123-134.

[17] **Jacob,A.M., Holzmann,W.** and **McCarthy,J.M.**, 1985. On Grasping Planar Objects with Two Articulated Fingers . İEEE J. of R and A, Vol 1(4) ;

[18] **Jacobsen,S.C., Johnson,R.T.** and **Biggers,K.B.**, 1986. Design of the Utah / MIT Dextrous Hand . İEEE Trans. of R and A ; pp. 1520-1531.

[19] **Ji,Z.** and **Roth,B.**, 1988. Direct Computation of Grasping Forces for 3-finger tip prehension grasps . ÀSME J. of Mech.,Trans. and Automation in Design, Vol 110 ; pp 405-413.

[20] **Kahng,J.** and **Amirouche,F.M.L.**, 1987. Impact Force Analysis in Mechanical Hand Design . Proc. of IEEE Int. Conf. on R and A.

[21] **Kerr,J.** and **Roth,B.**, 1986. An analysis of Multi-fingered Hands . İnt. J of Robotics Res., Vol 4(4) ; pp. 3-17.

[22] **Kumar,V.** and **Waldron,K.J.**, 1988. Force distribution in closed kinematic chains . İEEE J. of R and A, Vol 4(6) ; pp. 657-664.

[23] **Lakshminarayana, K.**, 1978. Mechanics of Form Closure . ÀSME Paper 78-DET-32 ; pp. 2-8.

[24] **Li,Z., Hsu,P.** and **Sastry,S.**, 1989. Grasping and Coordinated Manipulation by a Multifingered Robot Hand . İnt. J. of Robotics Res., Vol 8(4) ; pp. 33-50.

[25] **Lily,K.W.** and **Orin,D.E.**, 1994. Efficient dynamic simulation of Multiple Chain Robotic Mechanisms . J. of Dynamic Sys, Measurement, and Control, Vol 116 ; pp 223-231.

[26] **Mason,M.T.** and **Goldberg,K.Y.**, 1988. Planning Sequences of squeeze-grasps to Orient and Grasp polygonal objects . CMU-CS, Technical Report 88-127, CMU, Pittsburgh.

[27] **Mason,M.T.** and **Salisbury,J.**, 1985. Robot Hands and the Mechanics of Manipulation . MIT Press, Cambridge, Massachusetts.

[28] **Markenscoff,X.** and **Christos,D.**, 1989. Optimum Grip of a Polygon . Int J. of Robotics Res., Vol 8(2) ; pp. 44-61.

[29] **Markenscoff,X., Ni,L.** and **Papdimitriou,C.H.**, 1990 The geometry of grasping Int J. of Robotics Res., Vol 9(1) ; pp. 61-74.

[30] **Mukherjee,S.** and **Waldron,K.J.**, 1992. An Exact Optimization of interaction forces in 3-fingered manipulation . ASME J. of Mech. Design, Vol 114(1) ; pp. 48-54.

[31] **Murray,R.** and **Sastry,S.S.**, 1989. Control Experiments in Planar Manipulation and Grasping . Proc. of IEEE Int. Con. on R and A ; pp. 624-629.

[32] **Nakamura,Y., Nagai,K.** and **Yoshikawa,T.**, 1989. Dynamics and stability in coordination of multiple robotic systems . Int J. of Robotics Res., Vol 8(2) ; pp. 44-61.

[33] **Nguyen,V.D.**, 1986. The Synthesis of Stable Force-Closure Grasps . MIT AI lab, Technical Report 905, MIT, Cambridge.

[34] **Ohwovoriole,M.S.**, 1980. An Extension of Screw Theory and its application to the automation of industrial assemblies . Ph.D Thesis, Department of Mech Engg., Stanford University.

[35] **Park,Y.C.** and **Starr,G.P.**, 1990. Grasp Synthesis of Polygonal Objects . Proc. of IEEE Int. Conf. on R and A ; pp. 1574-1580.

[36] **Pollard,N.S.** and **Lozano-Perez, T.**, 1990 Grasp Stability and Feasibility for an arm with an articulated hand Proc. of IEEE Int. Conf. on R and A ; pp. 581-585.

[37] **Salisbury,J.** 1982. Kinematic and force analysis of articulated hands . Ph.D Thesis, Department of Mech Engg., Stanford University.

[38] **Salisbury,J.** and **Craig,J.J.**, 1982. Articulated Hands - Force Control and Kinematic Issues . Int J. of Robotics Res., Vol 1(1) ; pp. 4-17.

[39] **Selig,A.J.** and **Rooney,P.K.**, 1989. Realeaux pairs and surfaces that cannot be gripped. Int J. of Robotics Res., Vol 8(5) ; pp. 79-87.

[40] **Trinkle,J.C.**, **Abel,J.M.** and **Paul,R.P.**, 1987 An investigation of frictionless enveloping grasping in the plane . Int. J. of Robotics Res., Vol 7(3) ; pp. 33-51.

[41] **Wang,Y.** and **Mason,M.**, 1987. Modeling Impact Dynamics for Robotic Operations . Proc. of IEEE Int. Conf. on R and A ;

[42] **Yoshikawa,T.** and **Nagai,K.**, 1987. Manipulation and Grasping forces in Manipulation by Multi-fingered Hands . Proc. of IEEE Int. Conf. on R and A ; pp. 1998-2004.

[43] **Youcef-Toumi,K.** and **Li,D.**, 1987. Force Control of Direct-Drive Manipulators for surface following . Proc. of Int. Conf. on R and A ;

[44] **Zheng,Y.F.** and **Hemami,H.**, 1984. Impact Effects of Biped contact with the Environment . IEEE Trans on System, Man and Cybernetics, SMC-14(3) ; pp. 289-307.